A Thesis

Entitled

A Preliminary Numerical Investigation of Heat Exchanger Piles

By

Khagendra Kandel

Submitted to the Graduate Faculty as partial fulfillment of the requirements for the

Master of Science Degree in

Civil Engineering

Dr. Liangbo Hu, Committee Chair

Dr. Brian W. Randolph, Committee Member

Dr. Eddie Y. Chou, Committee Member

Dr. Amanda Bryant-Friedrich, Dean
College of Graduate Studies

The University of Toledo

August 2017

An Abstract of

A Preliminary Numerical Investigation of Heat Exchanger Piles

by

Khagendra Kandel

Submitted to the Graduate Faculty as partial fulfillment of the requirements for the
Masters of Science Degree in
Civil Engineering

The University of Toledo
August 2017

Heat exchanger piles are the thermo-active foundation system that can be used to extract geothermal energy for heating and cooling in the supported upper structures. Geothermal energy is a renewable, clean, efficient and cost-effective source of energy. The temperature below the Earth's surface remains relatively constant throughout the year but varies spatially with the earth depth. Piles are typically used as a main component of engineering structures, transferring the load from an upper structure to the supporting geological formation when necessary. The temperature gradient can be utilized by facilitating a circulating fluid inside the pile which can extract heat from the ground as well as release the heat to the ground during winter and summer seasons, respectively. As such these so-called heat exchange piles serve as both a structural component as well as a heat exchanging component.

The main objective of this thesis is to numerically study the behavior of heat exchanger piles and surrounding soils under different scenarios. Different combinations of thermal, mechanical and hydraulic loadings were applied during the simulation of the heat exchanger pile using a finite element program, Code_Bright. Mechanical responses of the

heat exchange pile were examined, along with the thermal and mechanical responses of soils. Some hydraulic scenarios were also explored.

First, numerical simulations were carried out under the mechanical loading only, focusing on the thermo-mechanical behavior of heat exchanger pile. The mechanical properties of the pile were examined and the compressive stress was found to be maximum at the pile head and decrease along the pile depth during the application of the pure mechanical loading; whereas during the application of thermal loading with the mechanical loading, the compressive stress was found to be maximum around the mid-depth of the pile with minimum values at the ends. The point of maximum stress, referred as the point of inversion or null point, coincides with the same point from which the vertical displacement and shear stress change direction. The behavior of the soil surrounding the heat exchanger pile was also examined, in particular, the investigation was focused on the radial range of soil within which the soil response was considerably affected.

Secondly, hydraulic scenarios were also explored in the context of potential thermo-hydro-mechanical processes the surrounding soil likely undergoes. The distribution of mechanical responses such as vertical stresses, vertical strains and vertical displacements were found to be similar to those under the thermo-mechanical loading but their magnitudes were affected. The influencing distance in the surrounding soil also varies substantially from the thermo-mechanical loading.

Acknowledgements

I would like to express my deepest gratitude to my advisor, Dr. Liangbo Hu, under whose supervision this thesis has been accomplished. His continuous advice, patience, encouragement and guidance throughout my research were indispensable.

I am grateful to the College of Graduate Studies and the Department of Civil Engineering for providing me the opportunity to Pursue my Master's Degree.

I would like to express my gratitude to my committee members, Dr. Brian W. Randolph and Dr. Eddie Y. Chou for their valuable suggestions and guidance during this research work.

I am thankful to my friends and family for their continuous support during my coursework and research.

Table of Contents

List of Tables

List of Figures

List of Abbreviations

GHP ……………………………….. Geothermal Heat Pump

kN……………………………...... Kilo Newton

M …………………………………. Mechanical

m …………………………………. Meter

MN…………………………………. Mega Newton

MPa…………………………………Mega Pascal

T …………………………………. Thermal

THM ………………………………. Thermo-Hydro-Mechanical

TM…………………………………Thermo-Mechanical

List of Symbols

The following notations will be used in balancing equations:

ΔT……………………………….Change in Temperature
θ………………………………mass content per unit volume of phase, i.e., $\theta=\omega\rho$
ρ………………………………density
$\boldsymbol{\sigma}$………………………………stress tensor
Φ………………………………Porosity
ω………………………………mass fraction
^{o}C…………………………….. Degree centigrade

$\mathbf{b}$………………………………body forces
E………………………………specific internal energy
$\mathbf{i}$……………………………….non-advective mass flux
$\mathbf{i}_c$…………………………....conductive heat flux
$\mathbf{j}$……………………………….total mass flux
$\mathbf{j}E$……………………………...energy fluxes due to mass motion
$\mathbf{q}$…………………………….....advective flux
S_l, S_g……………………….....degree of saturation of liquid and gaseous phases i.e., fraction of pore volume occupied by each phase.
$\mathbf{u}$……………………………….solid displacements

Chapter 1

Introduction

1.1 General Background

Geothermal energy is coined from two Greek words, 'Geo' means earth and 'thermos' means hot, which refers to the energy derived from the Earth's heat. It is a clean, cost effective, sustainable and environmentally friendly source of energy. We can find a wide range of examples for the extraction of geothermal energy, varying from a shallow ground to hot water and hot rock which can be found a few miles beneath the Earth's surface and the extremely hot molten rock called magma at the earth core. The soil below a few meters, generally 8-10 m, from the earth surface always remains at the same temperature, which is the main source of energy in geothermal applications, whereas the temperature at the earth surface keeps on changing from season to season. Figure 1-2 shows the variation of temperature on the earth's surface throughout the year, which can be used in the analyzing of potential geothermal energy. The underground reservoirs of steam and hot water can be tapped to generate electricity or to heat and cool buildings directly. The method of using the constant temperature below the earth surface either for heating of buildings during winter or cooling of buildings during summer is usually referred to as the extraction of geothermal energy. Hot springs are the most convenient example in the use of geothermal energy, whereas the steam turbines are the most technological and advanced form for its use.

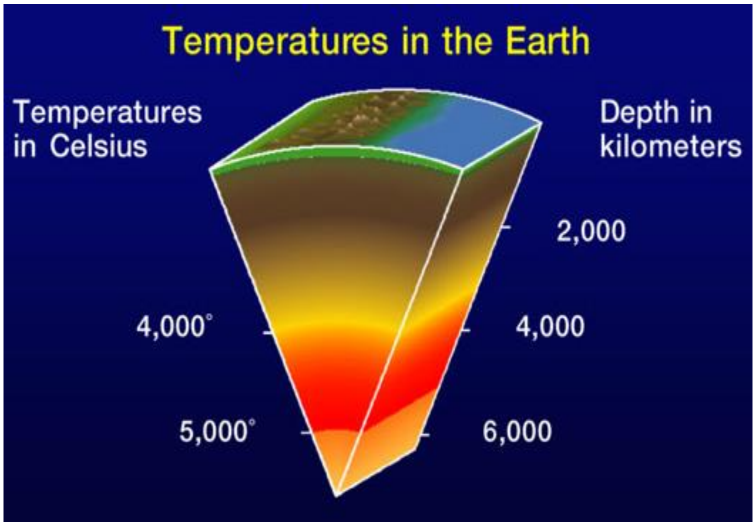

Figure 1- 1: Variation of mean earth temperature with the depth (Geothermal energy Association: http://geo-energy.org/Basics.aspx)

Historically, people began harnessing geothermal energy thousands of years before they had the technology to dig down into geothermal reservoirs. Romans used hot springs to heat their homes, bathe and cook in the beginning of human civilization. First modern district heating system of geothermal energy was developed in Boise, Idaho in 1892, where water pipes were used from the hot springs to heat the buildings. The first geothermal energy plant was built in Larderello, Italy in 1904. Nowadays, almost every country in the world uses geothermal energy. United States, Japan, New Zealand, France, Turkey, Germany and Iceland are among the most active in the exploitation of geothermal energy. Iceland is the country known as most dependent on geothermal energy. For example, the entire city of Reykjavik is heated with geothermal wells and hot springs. In United States, most of the geothermal reservoirs of hot water are located in the western states, Alaska and

Hawaii. The western states of USA are utilizing geothermal energy with a maximum consumption in California, 80.7% of the total consumption in the United States.

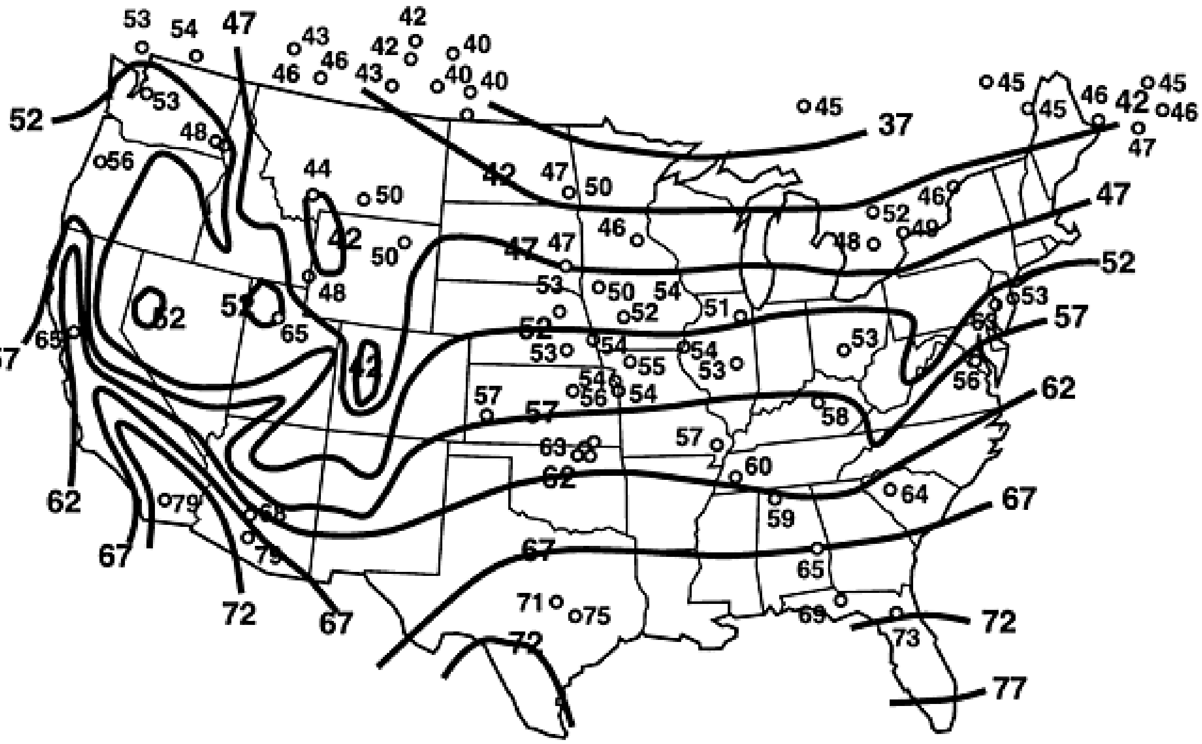

Figure 1- 2: Mean Annual ground temperature in different parts of United States (http://www.builditsolar.com/Projects/Cooling/EarthTemperatures.htm)

The use of geothermal energy can be categorized as direct use and indirect use. Direct applications include the heating or cooling of buildings, growing plants in greenhouse, drying crops, heating water at fish farms, snow melting and so on. As an indirect use, geothermal energy can be used as a source for electricity production. There are many scientific technologies involved in the use of geothermal energy, e.g. geothermal heat pump (GHP) is a device used in heating and cooling of the building.

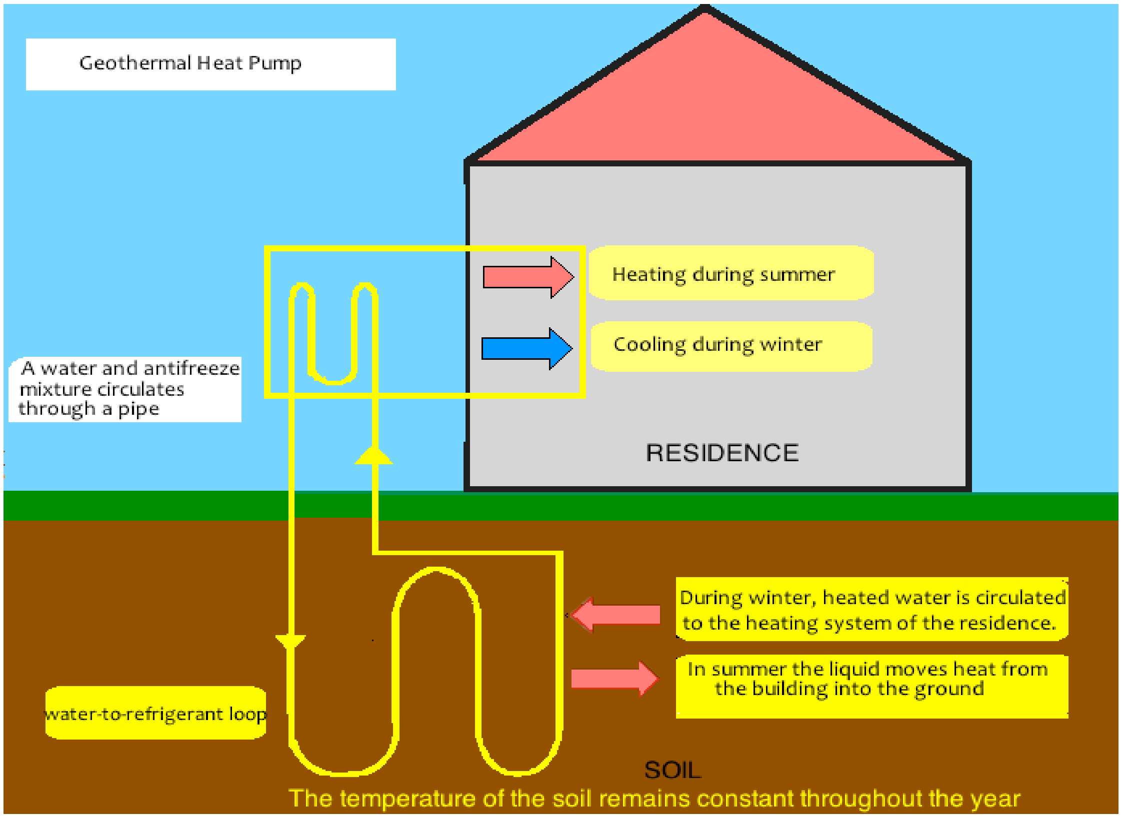

Figure 1- 3: Building heating and cooling from geothermal energy (https://rampages.us/kimpetersfocusedinquiry/2015/11/18/geothermal-energy/)

1.2 Geothermal Heat Pump (GHP)

Geothermal heat pump or ground-source heat pump (GHP) is a central heating and/or cooling system that is used to transfer heat to or from the ground. GHP uses the ground heat as the source of heating or cooling of the building. The temperature around the earth surface varies from season to season but at some depth below it the temperature is constant throughout the year. It uses the earth as a heat source during the winter and a heat sink during the summer. In the heating cycle, the temperature of the earth is higher than the surrounding temperature, so the earth can be used as a heat source to extract the heat while during the cooling cycle the temperature of earth becomes lower than the atmospheric temperature so earth can be treated as a heat sink. Generally, water filled polyethylene pipes are used as a heat exchanging medium between the ground and heat pump system. Omer (2008) stated that the GHP can reduce the emission of greenhouse gas by more than 66% as compared to the traditional methods of heating and cooling. A GHP system consists of three primary parts: the heat exchanger pipes, the heat pump and the heat distribution system. Heat exchangers are high density polyethylene pipes filled with water (sometimes mixed with antifreeze) as heat transfer fluid and they are mainly horizontally and vertically distributed. The heat pump removes heat from the heat exchanger and pumps it into the heat distribution system during the winter, while in the summer the process is reversed where the heat pump moves heat from indoor air to the heat exchanger system. Figure 1-3 shows the schematic diagram for the direct use of geothermal energy for the purpose of maintaining the building temperature throughout the year.

1.1 Heat Exchanger Piles

Heat exchanger pile is the indirect application of geothermal heat energy where the ground heat is used in gaining and losing the temperature from and to the ground. Concrete can be used as an ideal material for harvesting the heat from the ground since it has a good thermal conductivity and thermal storage capacity. Polyethylene pipes are inserted in the pile reinforcement cage during the construction of a heat exchanger pile which can be filled with heat exchanging media. The concrete forming the piles provides an ideal energy transfer medium, which allows the energy derived from the ground to be used in the heating and/or cooling of the structure. Photos of geothermal pile can be seen in Figure 1-4. The first picture shows the bar binding with a polyethylene tube inserted in the pile whereas the second shows a picture after the construction of foundation with fluid flowing pipes.

Figure 1- 4: Sample images of geothermal heat exchanger pile
(http://www.archiexpo.com/prod/haka-gerodur/product-62315-396403.html)

1.2 Objective

Geothermal energy has been used as a source of alternative energy for many years, which is a cost effective, reliable, clean and sustainable type of natural resource. It can be used either as a direct source of energy or indirect source of energy. As a direct source, it can be used in heating buildings, raising plants in greenhouse, drying crops etc. As an indirect use, it can be used in electricity production, heat exchanger piles etc. Improved understanding of the behavior of energy piles is still much needed for a more widespread use of geothermal energy. A proper design and construction of heat exchange piles should take into account the effects of complex thermal, mechanical and possibly hydraulic interactions involved in the response process of piles and soils, in addition to the bearing capacity and settlement in conventional piling and foundation design. The present study addresses some of the uncertainties in the soil-pile interaction in heat exchange piles through simulations of a single energy pile surrounded by soil undergoing combinations of multi-physics processes. The main goals of this research are:

1. To investigate the mechanical response of energy piles in different loading conditions.
2. To assess the behavior of soil foundations, in particular, the influencing distance of energy piles in the soil.

1.3 Thesis Outline

The content of this thesis is primarily focused on the mechanical behavior of heat exchanger piles under different types of loadings. The effects caused on soil due to the load application on the pile are also focused on this thesis. A literature review of heat exchange piles is discussed in Chapter 2.

In Chapter 3, the behavior of pile and soil due to the application of thermo-mechanical loadings is analyzed; the simulation process implemented in the finite element program is presented.

Chapter 4 deals with the behavior of the pile exchanger and the surrounding soil which undergoes the thermo-hydro-mechanical (THM) processes. Coupled THM modeling of soil is discussed in this chapter.

Chapter 5 presents the conclusion of the thesis with some recommendations for future research.

Chapter 2

Literature Review

2.1 Introduction

In the recent years, there has been a growing interest in geothermal energy and heat exchanger piles around the world. Some of the most important research projects in this area are discussed in the following section.

2.2 Previous Works Related to Heat Exchanger Piles

Laloui et al. (2006), conducted a study of an end bearing heat exchanger pile to compare the in-situ tests and results of coupled multi-physical finite element modeling. The field tests were carried out at the Swiss Federal Institute of technology (four story building) in Lausanne, Switzerland. The drilled heat exchange pile was 25.8 m in length and 88 cm in diameter. A coupled thermal-hydro-mechanical finite element model was developed and a single pile subjected to thermal loading, and thermal and mechanical loadings were analyzed. The soil was modeled as a Drucker-Prager thermo-elastic-plastic material while the Heat Exchanger Pile was assumed to behave as a thermo- elastic material. The contact between the pile and soil was assumed to be perfectly rough and the Heat Exchanger Pile was embedded into a soil profile consisting of 4 different layers, which are underlain by the bedrock. The pile was subjected to two different types of loads individually and combined i.e. mechanical loading only, thermal loading only and the combination of both mechanical and thermal loading. Different mechanical behaviors of a pile during individual and combined loadings were observed. Mechanical behaviors like axial stress and axial strain were the focus of study in this paper. The results from their experiments indicated that at the end of heating cycle large axial stress was obtained at the pile tip which is due to the uniform nature of the thermal effects, while axial stress was noticed at the pile top when the mechanical load was applied on the pile. The results from this paper show that either stress or strain produced on the soil-pile interface due to mechanical and thermal loading was the superposition of the individual loading. Though the thermal effect propagates highly in the soil as compared to mechanical load, the induced strains were limited and did not affect the pore water pressure.

A thermo-mechanical model was presented by Ozudogru et al. (2015) to study the behavior of pile in the variation of different temperature and loadings. An interface element was introduced between the soil and pile to study its behavior in loadings and its effect on the mechanical behavior of pile. The interface element was used to interpret the slip displacements and shear stresses along the soil-pile contact interface of a free top floating pile subjected to elevated temperatures. The main concentration of this study was on the thermo-mechanical stress developed in the pile upon the temperature increment. The temperature of the surrounding soil was assumed to be constant while pile was heated uniformly and the results of axial stress, shear transformation, and slip displacement were studied for different temperature change in the pile. The results of this study indicated that the total strain or stress that the pile feels in the sum of both mechanical and thermal effects while the interface element introduced between the soil and pile does not play any role in the thermal stress and strain of the pile. The pile encounters friction at the interface with soil during the thermal loading which is verified by the result of stress variation in the pile with mechanical loading only and the thermomechanical loading. Because of the friction, the maximum stress could be obtained at around the mid-depth of the pile, referred as the neutral point, during thermomechanical loading whereas maximum stress was obtained at pile top with the effect of pure mechanical load. The neutral point would have been at the mid-depth of the pile if it was set free to expand in both directions but because of soil on the pile tip, neutral points shifts some downward from the mid-length. The heat exchanger pile was first studied with the free top to investigate the magnitude of internal thermo-mechanical stresses that had developed in the pile in reaction to the induced temperature increase and it showed that the soil-pile interaction was directly influenced by the interplay between the thermal strains in the pile and the associated shear stresses developed along the soil-pile interface. In the analysis followed the first, pile was fixed on the top and the total stress increment was observed and the result showed that the constrained vertical elongation was the most detrimental factor for the pile foundation performance. Furthermore, it should be noticed that the mechanical constraints (e.g., fixed top and/or fixed bottom) require oversizing heat exchanger piles at the ends and the interface effects require additional reinforcing the pile at mid-depth. Moreover, from the analysis presented in this paper, it could be suggested that no significant gain of foundation performance was achieved because of friction upon pile heating.

Bourne-Webb et al. (2009) presented the behavior of energy pile during the heating and cooling process on the geotechnical performance of piled foundations incorporating pipe loops for ground source heat pump system. This paper was based on the data collected during the field tests on the energy piles located at the Lambeth College in London. The field test was designed to investigate the behavior of energy piles which were subjected to either thermal loading only or the combination of both thermal and mechanical loading. The mechanical behaviors of pile such as the pile head displacement, temperature and strain along the pile were observed during the initial mechanical loading, at the end of first heating period as well as at the end of first cooling period. Optical Fiber sensors, vibrating wire strain gauges and thermistors were used to record the data for the axial response of the test pile. There were 18 vibrating wire strain gauges (VWSG), 6 thermistors and five external load control elements for the pile tests were used to record the data on the energy piles which were used to determine the axial stresses in the pile.

The test pile was designed with a diameter of 610 mm on the upper 5 m depth while the diameter was reduced to 550 mm on the lower 18 m. It was designed to carry the vertical load equivalent of 1200 kN as the working load. The temperature applied during the thermal test period varied from -6^{o}C to 56^{o}C. The range of temperature change represented the extreme case where during the cooling of pile it was intended to make a freezing environment at the soil pile interface.

The test pile under consideration experiences the thermal stress both in heating and cooling mode but the nature of thermal stress is opposite in each case i.e. during the heating of energy pile it expands whereas during cooling mode the pile contracts. Under the thermal loading the expansion or contraction of pile occurs at about the mid-depth of the pile which is termed as a ‘null’ point.

Amatya et al. (2012) concluded that in the thermodynamic design of the ground source heat pump system the pile acts as an infinitely long heat source and it emits the temperature in all directions. They also concluded that the stresses in the test pile were induced due to the mechanical loading while the pile was heated could exceed the limiting value imposed by the design codes. They also found that the stress mobilized at the soil-pile interface will significantly affect to the overall bearing capacity of energy piles.

Amatya et al. (2012) synthesized the published pile test results that involve three different sites. They developed simplified load transfer mechanisms for thermal, and combined thermal and mechanical loads for a single pile. Specifically, they focused on the change in axial stress, mobilized shaft resistance of energy piles in response to heating and cooling, and effects of end restraints.

One of the field tests took place at the grounds of Clapham Center of Lambeth College in South London. Two piles were constructed at the site, a 23 m long test pile and 30 m long heat sink pile. The mechanical load of 1200 kN was applied on the main test pile and was maintained for 46 days. The test pile was subsequently cooled for 31 days, which was followed by heating for 12 days. Finally, the pile was heated and cooled in daily cycles lasting three days.

The second test site was located at the E´cole Polytechnique Fe´de´rale de Lausanne (EPFL) in Lausanne (Switzerland). The pile under consideration was located at the edge of a four-story building, which was under construction during the period of testing and served both as a load bearing member and energy exchanger. A 28 days thermal testing was performed with a different head load firstly without any external load on the pile head followed by a load of 1300 kN.

The location of the third field test was Bad Schallerbach, Austria. The test pile was a part of piled raft which supported a seven-story building that was benched into a sloping site and the pile was equipped with pressure cells at the toe and the head, ‘fissuremeters’ at three levels, and ‘thermo-elements’ at five levels. Data were collected intermittently at different times of the year over several years’ operation of the system. The pile has a diameter of 1.2 m and the length of 9 m.

Amatya et al. (2012) concluded that during the heating and cooling cycles, energy piles expand and contract which changes the soil-pile interaction. Furthermore, heating and cooling of the piles induced the axial stress inside the pile, which was between about 50% and 100% of the theoretically fully restrained values. Although they found that stiffer soils seem to exhibit larger mobilization of shaft resistance they also indicated that methods for estimation of these effects needed to be developed. Finally, they stated that the heating and cooling of energy piles are not likely to have detrimental effects on buildings.

Rotta Loria et al. (2015**)** presented the analysis of the thermo-mechanical behavior of energy pile foundation in saturated soil to expand the effects of different magnitudes of monotonic heating loads and axial mechanical loads which were applied prior to the temperature change. The focus of the study was to observe the impact of different magnitudes and combinations of thermal and axial mechanical loads on the mechanical behavior of energy piles. The results obtained from a series of thermo-hydro-mechanical finite element analysis were compared with centrifuge data and parametric numerical runs. The finite element analyses were performed at the Swiss Federal Institute of Technology in Lausanne, whereas the centrifuge tests were performed at the Geotechnical Centrifuge Facility of the Hong Kong University of Science and Technology.

The finite element analysis was performed by considering a representative pile foundation capable of exchanging heat with the surrounding saturated ground and subjected to a mechanical vertical load. All three aspects of loading i.e., mechanical, thermal and hydraulic loading were involved during the analysis where the equilibrium and balance equations and the water and heat diffusion laws were expressed in the moving current configuration using a Lagrangian-updated formulation.

This paper suggests that the higher mechanical and thermal loads on the energy piles induce larger stress which are ultimately transferred to the soil and the temperature insensitivity to centrifuge scaling does not affect the assessment of the mechanical response of energy piles through the considered experimental technique for the coarse-grained soil. For higher thermal and/or mechanical loads, plastic strain occurs at the soil-pile interface which induces a larger effective horizontal stress and affects the mechanism of side shear resistance mobilization of the pile and the null point depends on the magnitude of the thermal and mechanical.

Akrouch et al. (2016) presented a method to evaluate the heat exchange rate of energy piles in unsaturated soil condition. A parameter for thermal efficiency function (ζ) was proposed as the ratio of amount of heat exchanged when soil was unsaturated to the amount of heat exchanged when the soil was fully saturated. When the soil was fully saturated, the heat exchange rate was found to be maximum i.e. $\zeta = 1$. This research was mainly focused on the determination of average thermal efficiency ratio for different position of the water table and soil types. The ζ function was dependent on the soil thermal properties, the degree of saturation and the thermal resistance of the energy pile. The heating tests were performed under controlled temperature and constant water content conditions. The results obtained from finite element model was compared with analytical and experimental results and found a very good consistency with each other. It was shown that the performance of energy piles could drop up to 40% during the case of sand at a very low degree of saturation.

Suryatriyastuti et al. (2012) used finite difference code FLAC^{3D} to simulate an energy pile under static loading. They used two different computational models: one with perfectly rough contact and the other with sliding contact along the soil-pile interface. The pile was 15 m long and it has 0.6 m x 0.6 m square cross section. It was installed into the homogeneous soil. Both pile and soil were assumed to behave as the thermo-elastic materials. The soil deposit was 15 m in wide and 30m in high. The pile was heated to 25^{o}C and subsequently cooled to 5^{o}C.

Suryatriyastuti et al. (2012) concluded that the stresses and displacement obtained from sliding contact model were smaller than those obtained from perfect contact. The mechanical properties during heating cycle of the pile were opposite of those during cooling of the pile whereas the null point was located at the middle of the pile.

Gao et al. (2008) presented a case study of thermal performance of ground temperature of vertical pile-foundation heat exchangers to examine the geothermal energy for a district heating and cooling system in Shanghai, China. Several tests were performed to determine the most effective vertical pile foundation heat exchanger and a single pile foundation heat exchanger was found to be the most efficient one. They also evaluated a numerical result under two imbalance ratios between cooling and heating load to evaluate the potential of geothermal energy. Three dimensional numerical simulations for coupling heat convection and conduction through water in pipeline, concrete pile and soil, were performed to determine the most efficient type pile-foundation heat exchangers and the experimental data were used to validate the numerical results moreover numerical methods were used to determine the five-year variations of the ground temperature. The results of this study were supposed to be used for district heating system in Shanghai, China.

As a conclusion, J. Gao et al. (2008) stated that the W-shaped type of pile-foundation ground heat exchanger with moderate medium flow rate was found to be most efficient from both the experimental and numerical analysis and was finally applied in Shanghai, China. The water temperature descending in the pipe reduces the heat transfer potential from water in the pipe to the soil and it slightly decreases with the flow direction.

A numerical procedure for the simulation of heat and fluid flow in a heat exchange system for exploitation of low enthalpy geothermal reservoir was proposed by Carotenuto et al. (2012). They applied a generalized model for the mathematical description for heat and fluid flow through saturated porous media to study down hole heat exchanger, well and aquifer using a single domain approach. A study state operation of the system was considered and the results obtained were validated with the experimental data collected for a geothermal convector prototype installed in an existing geothermal well.

A Carotenuto et al. (2012) concluded that their method can be successfully used in the prediction of complex phenomena that occur in geothermal heat recovery system which had been used to verify some of the results observed with previous approximate model to gain the understanding of the interaction between down-hole heat exchangers, well and geothermal aquifers. They also suggested that the use of down hole heat exchangers

(DHEs) are not implacable for moderate values of heat flow rate need to be withdrawn from aquifers with low natural fluid circulation.

You et al. (2014) presented an In-situ experimental study of heat exchange capacity of cement-fly ash-gravel (CFG) pile geothermal exchangers. An in-situ full-scale study was carried out using the thermal response test and thermal performance test to investigate the heat exchange capacity of the CFG piles usually used in foundations for low to medium high-rise buildings in Beijing. This paper analyses the influence of the hydration heat of cement, heating power, inlet water temperature, circulation water flow velocity, operation mode, and group pile effects on the heat exchange capacity of CFG pile geothermal exchangers. From the investigation of heat exchange capacity of CFG single piles and grouped piles using an in-situ full-scale experimental method S You et al. (2014) suggested that the hydration heat of CFG pile is gradually released over five to six days until pile temperature returns to the surrounding soil temperature. Moreover, the heat exchange rate of a CFG energy pile is positively proportional to the inlet water temperature under the thermal performance testing condition and the heat injection rate of group piles decreases by 5% and the heat extraction rate decreases by 20 % as compared with the single pile. CFG piles should be arranged at a spacing of no less than 8 m since the temperature influence radius of a single CFG pile exceeds 4 m.

Mimouni & Laloui (2015) and Ã & Laloui (2016) made a research under the behavior of energy piles when they are applied in a group. A full-scale lab set up was built on the main campus of the Swiss Federal Institute of Technology in Lausanne, Switzerland. Pile groups are classified as widely spaced and closely spaced according to the spacing between the piles and the effect of a pile on another. The effect that occurs in an energy pile due to thermal or mechanical loading on the adjacent pile is termed as group effect on these research articles. From the laboratory experiment and numerical analysis, Rotta Loria and Laloui (2016) concluded that the thermal and thermally induced mechanical interactions must be considered during the analysis and design of energy group piles whereas the linear thermo-elasticity theory was proposed as the sufficiently accurate tool to describe the geotechnical and structural behavior of a wide number of energy pile groups for research as well as engineering designs. Mimoui and Laloui (2015) stated that the pile-structure-pile interactions were investigated as the heated pile pulled on the adjacent piles, from pile heads to pile bases. During the simultaneous heating test of a group of energy piles, significant group effect can be observed when comparing with the pile thermomechanical response during the group test and the single pile test. Moreover, the degree of freedom was doubled and the pile heaving was increased due to great induced thermal strains and the differential displacement between the test piles was reduced because of the group effect of piles.

For the analysis of geotechnical scenarios, different geotechnical software packages are in use. In this research Code_Bright, a finite element software, has been used. Geotechnical finite difference numerical software, FLAC can be used for modelling different geological aspects, geothermal analysis and geotechnical hazard analysis (Rawal et al., 2017; Rawal et al., 2016; Wang et al., 2017; Wang et al., 2016).

2.3 Summary

The literature review presented in this chapter shows that the majority of existing research about heat exchange piles has been primarily focused on the thermal effect on the mechanical response of the pile and its implication on pile design aspects, whereas the soil response has not been extensively investigated, especially under potentially complex scenario of soil undergoing coupled thermal, mechanical and hydraulic processes. The consideration of behavior of partially saturated soils may also become inevitable in these scenarios. In this research, numerical simulations of some complex scenarios are conducted to better understand the behavior of heat exchange piles and surrounding soils.

Chapter 3

Thermo-mechanical Behavior of a Heat Exchanger Pile and Surrounding Soil

3.1 Introduction

To simulate the behavior of heat exchanger pile and the surrounding soil, a numerical model coupling the mechanical behavior to the thermal phenomena is required. The problem considered in this case is a pile foundation that is capable of exchanging heat with the surrounding soil and subjected to mechanical vertical loading. In this analysis, a soil mass of 20m x 20m is considered with a pile of depth 15m and width of 0.5m; the entire domain is axisymmetric about y-axis under 3D consideration.

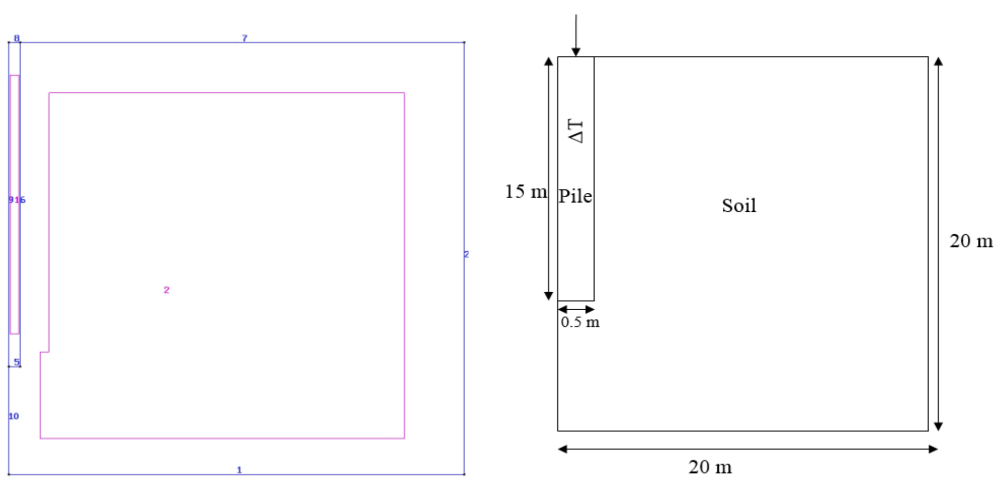

Figure 3- 1: A typical simulated domain consisting of a heat exchange pile and surrounding soil

A finite element analysis program, CODE_BRIGHT is used in the numerical simulations presented in this thesis. It was developed at the Universat Politecnica de Catalunya, Barcelona, Spain in late 1980s with features tailored toward the simulation of partially saturated soils.

Since the problem considered in this chapter is associated only with the thermomechanical process, only stress equilibrium and energy balance equations are used in the analysis, but all governing equations including mass conservation are presented altogether in this chapter for a complete description.

3.2 Mathematical Formulation

Different approach of mathematical simulations can be established to analyze the nature and behavior of pile under different combinations of thermal, mechanical, hydraulic loading. The assumptions and aspects considered in the formulation of problem are:

- Thermal equilibrium between different phases of soils is assumed, which means the phases are at the same temperature.
- State variables (also called unknowns) are: solid displacement, $\boldsymbol{u}$ (in three spatial directions); and temperature, T.
- Balance of linear momentum for the medium is reduced to the equation of stress equilibrium together with a mechanical constitutive model to relate stresses with strains. Strains are defined in terms of displacements.
- Small strains and small strain rates are assumed for solid deformation.
- Physical parameters in constitutive laws are function of pressure and temperature

The equations that govern problem can be categorized into four main groups. These are: balance equations, constitutive equations, equilibrium relationships and definition constraints. Equations for mass balance are established following the compositional approach. Equation for balance of energy is established for the medium. The equation of momentum balance for the porous medium is reduced to that of stress equilibrium.

The following notation will be used in balance equations:

φ: porosity

ρ: density

j: total mass flux

θ: mass content per unit volume of phase, i.e., $\theta=\omega\rho$,

i: non-advective mass flux

q: advective flux

u: solid displacements

σ: stress tensor

b: body forces,

ω: mass fraction,

E: specific internal energy

$\mathbf{i}_c$: conductive heat flux

$\mathbf{j}_E$: energy fluxes due to mass motion

S_l, S_g: degree of saturation of liquid and gaseous phases i.e., fraction of pore volume occupied by each phase.

Superscripts *w* and *a* refer to water and air, respectively

Subscripts *s*, *l* and *g* refer to solid, liquid and gas phase, respectively.

3.2.1 Balancing Equations

These governing equations include: balance of linear momentum (stress equilibrium) equations (in 2D), mass balance equations (different species) and internal energy balance equation for the porous medium.

The stress equilibrium equations are a simplified form of the balance of linear momentum for the porous medium. Mass balance of water, solid and air are established. Since the assumption of equilibrium is made, the mass of each species as present in any phase (solid, liquid or gas) is balanced for the porous medium. In this way, one equation for each species is obtained. The equilibrium assumption implies that partition functions are required to compute the fraction of each species in each phase.

Each partial differential equation is naturally associated to an unknown. These unknowns can be solved in a coupled way, i.e., allowing all possible cross coupling processes that have been implemented, or, on the contrary, any uncoupled problem to obtain a single unknown can be solved.

3.2.2 Mass Balance of Solid

Mass balance of solid present in the medium is written as:

$$\frac{\partial}{\partial t}(\theta_s (1-\phi)) + \nabla (\mathbf{j}_s) = 0 \tag{1}$$

Where θ_s is the mass of solid per unit volume of solid and $\mathbf{j}_s$ is the flux of solid. From this equation, an expression for porosity variation was obtained as:

$$\frac{\mathrm{Ds}\ \phi}{\partial t} = \frac{1}{\theta s}\left[(1-\phi)\frac{\mathrm{Ds}\phi s}{\mathrm{Dt}}\right] + (1-\phi)\ \nabla .\ \frac{\mathrm{d}\mathbf{u}}{\mathrm{dt}} \tag{2}$$

The material derivative with respect to the solid had been used and its definition is:

$$\frac{\mathrm{Ds}(\bullet)}{\mathrm{D}t} = \frac{\partial}{\partial t} + \frac{\mathrm{d}\mathbf{u}}{\mathrm{dt}} .\ \nabla(\bullet) \tag{3}$$

Equation (2) expresses the variation of porosity caused by volumetric definition and solid density variation.

3.2.3 Momentum Balance for the Medium

The momentum balance reduces to the equilibrium of stresses if the internal terms are neglected:

$$\nabla .\boldsymbol{\sigma} + \mathbf{b} = \mathbf{0} \tag{4}$$

Where **σ** is the stress tensor and **b** is the vector of body forces.

3.2.4 Mass Balance of Water

Water is present in liquid an gas phases. The total mass balance of water is expressed as:

$$\frac{\partial}{\partial t}(\theta_l^w S_l \phi + \theta_g^w S_g \phi) + \nabla.(\mathbf{j}_l^w + \mathbf{j}_g^w) = f^w \tag{5}$$

Where f^w is an external supply of water. An internal production term is not included because the total mass balance inside the medium is performed. The use of the material derivative leads to:

$$\phi \frac{D_s(\theta_l^w S_l + \theta_g^w S_g)}{Dt} + \left(\theta_l^w S_l + \theta_g^w S_g\right)\frac{D_s \phi}{Dt} + \left(\left(\theta_l^w S_l + \theta_g^w S_g\right)\phi\right).\frac{d\boldsymbol{u}}{dt} + \nabla.\left(j_l'^w + j_g'^w\right) = f^w \tag{6}$$

The final objective is to find the unknowns from the governing equations. Therefore, the dependent variables will have to be related to the unknowns in some way. For example, degree of saturation will be computed using a retention curve which should express it in terms of temperature, liquid pressure and gas pressure.

Porosity appears in this equation of water mass balance not only as a coefficient, but also in a term involving its variation caused by different processes. It is also hidden in variables that depend on porosity (e.g. intrinsic permeability). The way of expressing the derivative term as a function of the state variables is via the solid mass balance equation. This allows to consider properly the influence of porosity variation in the balance equation for water.

It should be noted that in the last equation the material derivatives can be approximated as Eulerian if the assumption of small strain rate is performed while the volumetric change (porosity derivative and volumetric strain) is not neglected. This is the classical way of obtaining the coupled flow-deformation equations.

3.2.5 Internal Energy Balance for the Medium

The equation for internal energy balance for the porous medium is established taking into account the internal energy in each phase (E_s, E_l, E_g):

$$\frac{\partial}{\partial t}(E_s\,\rho_s\,(1-\phi) + E_l\,\rho_s\,S_l\,\phi + E_g\,\rho_g\,S_g\,\phi) + \nabla.\,(\mathbf{i}_c + \mathbf{j}_{ES} + \mathbf{j}_{El} + \mathbf{j}_{Eg}) = f^Q \tag{7}$$

Where $\mathbf{i}_c$ is energy flux due to conduction through the porous medium, the other fluxes ($\mathbf{j}_{Es}$, $\mathbf{j}_{El}$, $\mathbf{j}_{Eg}$) are advective fluxes of energy caused by mass motions and f^Q is an internal/external energy supply. In this case this term accounts, for instance, for energy dissipation due to medium deformation which is not explicit because it is negligible in most cases. The use of the material derivative allows one to obtain an equation formally similar to the mass balance of water. The reason for the similarity is that both water and internal energy, are considered present in the three phases.

Hence, only one equation is required which expresses the balance of internal energy in the porous medium as a whole. In problems involving geological materials, this equation usually reduces to the balance of enthalpy. The reason for this is that the variations of temperature produce enthalpy variations which are very large compared with the energy variations supplied from deformation work.

The fluxes in the divergence term include conduction of heat and advection of heat caused by the motion of every species in the medium. A non-advective mass flux causes an advective heat flux because a species inside a phase moves and transports energy. Contrary to what happens with the movement of a contaminant in a groundwater system, the diffusive term for heat transport (conduction of heat) is much larger than the term concerning hydro mechanical dispersion (non-advective flux caused by the velocity of fluids). For this reason, this term is usually neglected.

3.2.6 Boundary Conditions

Application of Green's theorem to the divergence term produces terms which represent fluxes or stresses across or on the boundaries. These terms are substituted by nodal flow rates or forces in the discretized form of the equations. For the mechanical problem, the classical approach is followed to impose external forces. Imposing displacement is made by means a Cauchy type boundary condition. The boundary conditions for the balance equations are incorporated by means of the simple addition of nodal flow rates. For the mass flow rate of water as a component of gas phase is:

$$J_g^w = (\omega_g^w)^0\, j_g^0 + (\omega_g^w)^0\, \gamma_g\, (P_g^0 - P_g) + \beta_g((\rho_g\omega_g^w)^0 - (\rho_g\omega_g^w)) \tag{8}$$

where the superscript $()^0$ stands for prescribed values. This general form of boundary condition includes three terms. The first one is the mass inflow or outflow that takes place when a flow rate of gas (j_g^0) is prescribed. Second term is the mass inflow or outflow that takes place when gas phase pressure (P_g^0) is prescribed at a node. The coefficient γ_g is a leakage coefficient, i.e., a parameter that allows a boundary condition of the Cauchy type. The third term is the mass inflow or outflow that takes place when vapour mass fraction is prescribed at the boundary. This term naturally comes from the nonadvective flux (Fick's law). Mass fraction and density prescribed values are only required when inflow takes place. For outflow the values in the medium are considered. For the energy balance equation, the boundary condition has a similar form.

3.2.7 Simulation Parameters

Initially the temperature is considered to be at a constant level for both soil and pile. Initial stress in assumed to be zero on both media with constraints on all sides except the top boundary. The vertical sides along the pile as well as on the soil deposit were constrained against the horizontal deformation whereas the bottom was constrained in the vertical direction. On the initial heating phase, the pile was free on the top and constrained at the bottom on the soil which creates positive and negative expansions. On the second phase, axial load is applied from the top of the pile. Only half portion of the pile is taken into consideration due to axisymmetry about y-axis. Typical values of material constants are presented in Table 3-1.

Table 3- 1: Material properties used in the simulation

Properties	**Units**	**Soil**	**Pile**
Young's Modulus (E)	MPa	70	10000
Poisson's ratio (ν)		0.3	0.2
Thermal conductivity of dry porous medium (λ_{dry})	Wm/K	1.0	1.5
Thermal conductivity of saturated porous medium (λ_{sat})	Wm/K	1.5	2.0
Solid phase specific heat (C_s)	J/Kg K	800	900
Solid phase density (ρ_s)	Kg/m^3	2100	2500
Linear thermal expansion coefficient for grains (α_s)	1/^{0}C	1.00E-05	7.80E-04

3.3 Numerical Simulations

In this chapter, the numerical simulations are focused on the response of the heat exchanger pile and surrounding soil under combinations of mechanical and thermal loadings.

3.3.1 Mechanical Loading Only

First, a simulation of mechanical loading without temperature change is conducted. A force varying from 1 MN to 4 MN is applied to the top of pile and the results are presented on the following section:

1. Vertical displacement in pile length

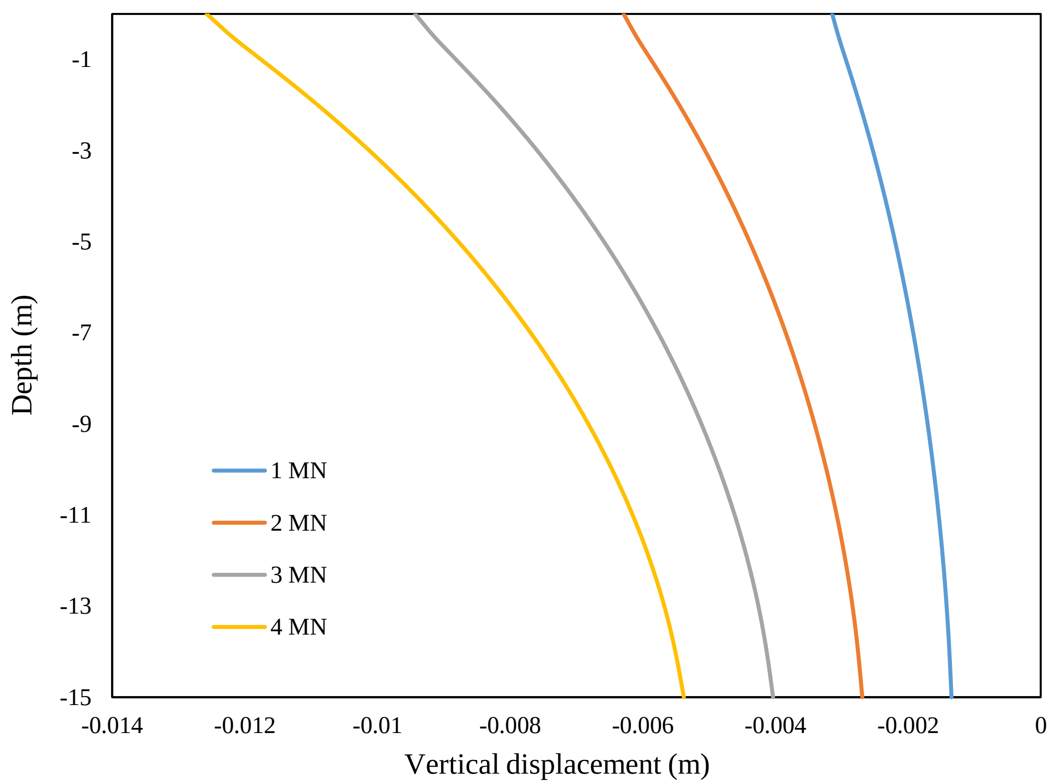

Figure 3- 2: Vertical displacement variation in the soil-pile interface on mechanical loading

Figure 3-2 shows the variation of displacement in vertical direction of pile when mechanical load is applied on the top. The downward displacement is clearly nonlinear across the depth. Since the mechanical loading is applied form the top of pile, the compression on pile is maximum at the top and decreases towards the bottom of pile.

Moreover, with increment of mechanical loads on the pile, the compressive vertical displacement increases i.e., the pile undergoes more compression.

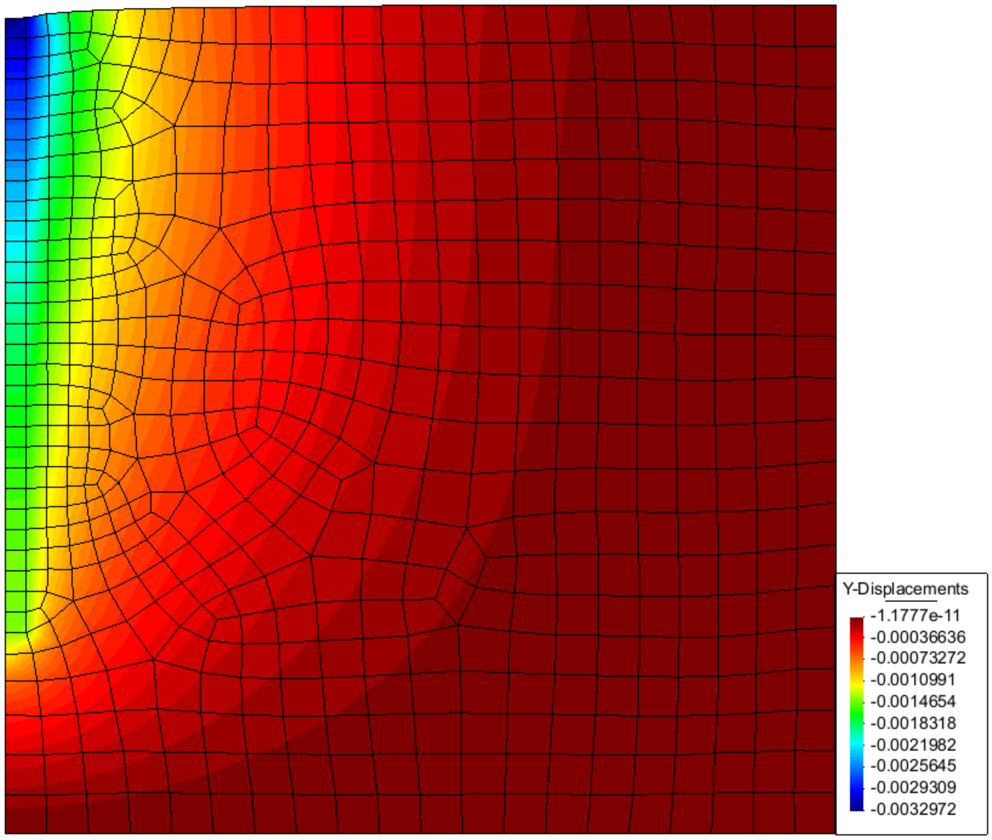

Figure 3- 3: The deformed shape for the vertical displacement variation

The deformed shape for the vertical displacement variation during the application of mechanical loadings is presented in figure 3-3. The figure shows that the pile goes on compression during the application of mechanical load on the pile. The soil away from the pile does not feel any compression but the soil around the pile is compressed because of the impact caused on the nearby area of the application of the load.

2. Axial stress distribution

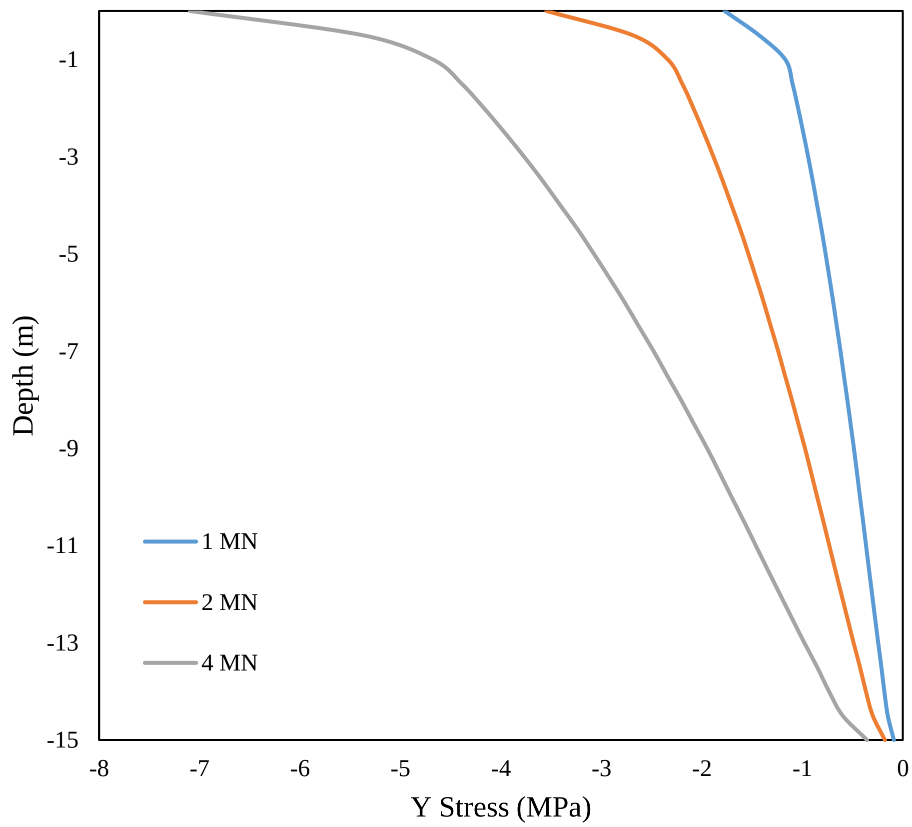

Figure 3- 4: Vertical stress distribution in the soil-pile interface on mechanical loading

The axial stress distribution due to mechanical loading is depicted in Figure 3-4. The maximum stress on pile due to mechanical loading occurs at the top of pile which decreases towards the bottom. The axial stress at the bottom of pile tends to be zero on any magnitude of loadings. This may be the cause of soil pile interaction as the stress is transferred to the ground to from the bottom of pile instead of resisting it. Figure 3-5 shows a stress distribution on soil pile interface with a soil with higher stiffness value. The stress produced in such a soil is in smaller amount than the weak soil which is the result of friction caused by the stiffer soil on the interface.

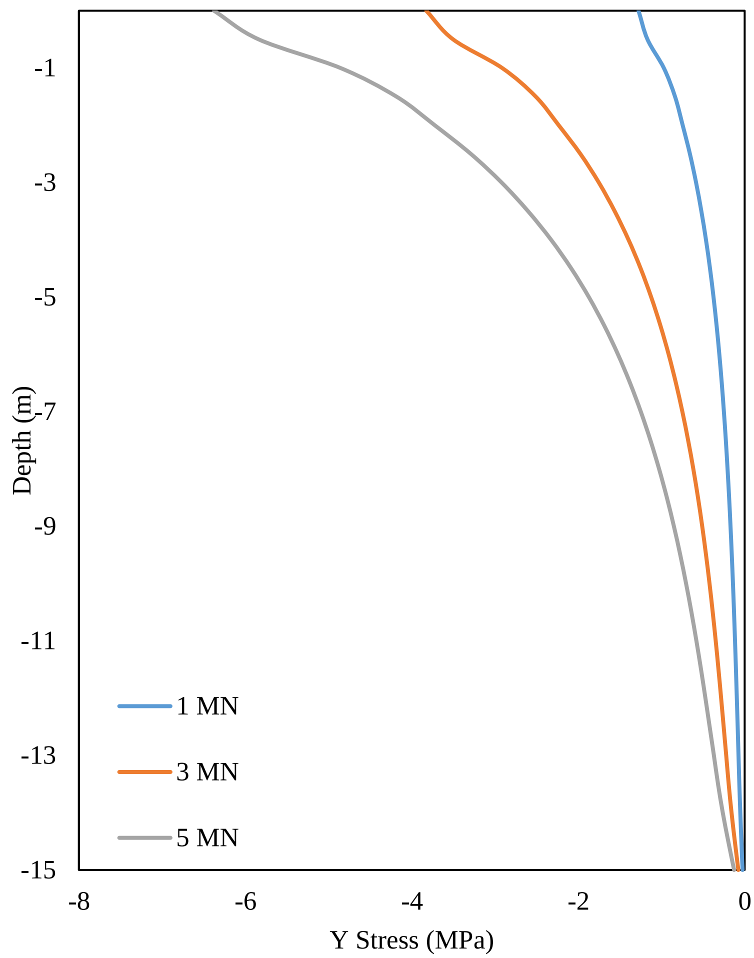

Figure 3- 5: Vertical stress distribution in the soil-pile interface with stiffer soil

3. **Shear Stress Distribution**

The shear stress distribution during the mechanical loading of a pile can be seen in figure 3-6**.** The shear stress is maximum at the top of the pile where the direct impact of applied load occurs. The shear stress almost becomes zero with the depth of the pile because the all the force applied from the top of the pile transfers to the ground so that the pile surface doesn’t encounter the frictional resistance with the soil.

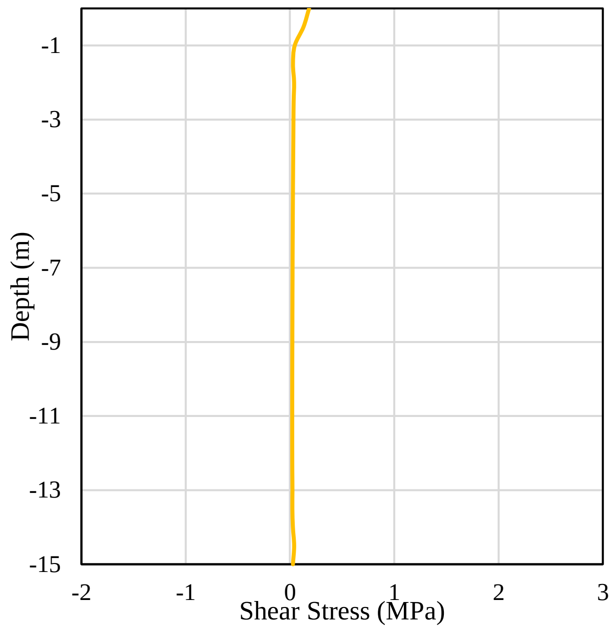

Figure 3- 6: Shear stress distribution during mechanical loading in the soil-pile interface

3.3.2 Thermal Loading Only

On this step of simulation, the temperature of pile was increased in a uniform rate from the initial temperature to a specific final temperature. Initially both the soil and pile were maintained at the same temperature of 20^{0}C and the pile was heated in a uniform rate. The rate of temperature increment in the pile can be seen in Figure 3-7. The color map in figure 3-7 shows the effect of temperature increment on the pile and the increasing temperature on the surround soil. On the beginning of simulation, both the pile and soil were maintained at a constant temperature (20°C) and the pile was uniformly heated to a desired maximum temperature. A 20 days simulation was carried out to raise the temperature on the pile to a final temperature as in the color map in figure 3-7. All the results presented in this section are the simulation results of 20 days' duration from the beginning.

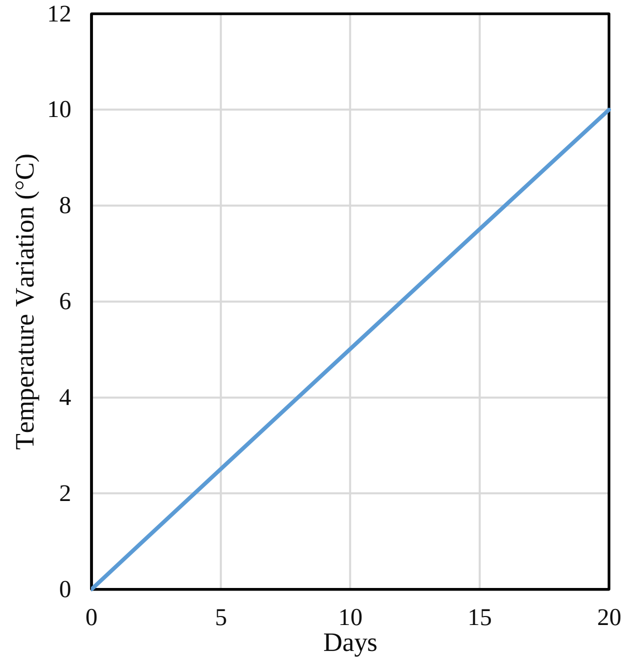

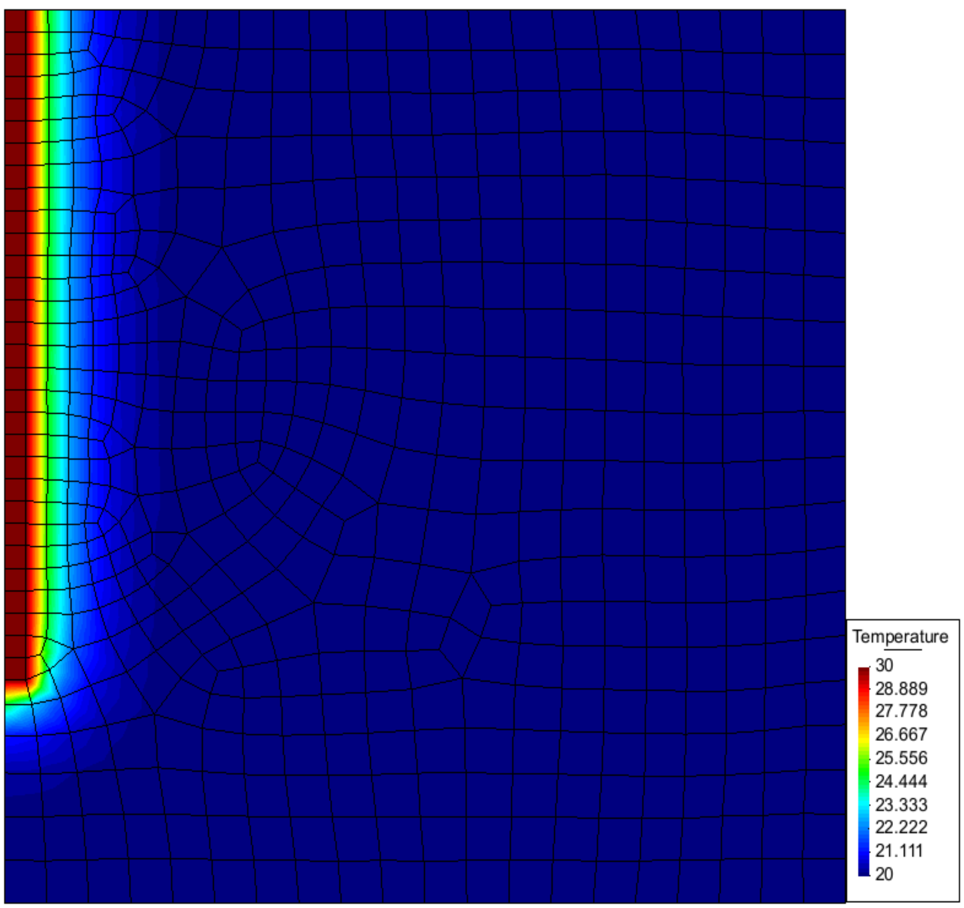

Figure 3- 7: Temperature increment in the pile under thermal loading

1. Vertical displacement

Figure 3-8 presents the vertical displacement under thermal loading. The top part of the pile expands upward when the temperature increases whereas the lower part i.e., near the toe of the pile, it tends to expand downward. Here the so-called neutral point of the pile, defined as the location where the expansion (displacement) of the pile would be zero, is below the mid length of pile and the upward expansion is more than the downward expansion. If the pile was set to expand freely, the neutral point would be at the center of pile length. but in this case the pile is not free to expand so the neutral point shifts downward because of the shear resistance of the soil at soil pile interface throughout the depth and below the toe of the pile. The neutral point is below the mid depth of pile i.e. around 9.10 m from the top of pile. Here the maximum upward displacement recorded due to the temperature change was found to be 0.05 m at the temperature increment of 10^0C which is equivalent to the total linear expansion value for the concrete with the assumed value of coefficient of linear expansion and the change in temperature for 15m depth of the pile. The color map in figure 3-8 shows the effect of temperature on the pile displacement, the figure shows the deformed shape of the pile after the increment of temperature by 10°C on the pile during the simulation of 20 days. As discussed, the top half of the pile goes on the upward expansion and the bottom half goes on downward expansion separating from the middle portion of the pile called the point of inversion or null point. The red part of the figure shows the upward expansion region while the blue color region shows the area of downward expansion. The soil on the periphery of pile faces some vertical expansion but away from the pile, the effect on the expansion is almost negligible and zero.

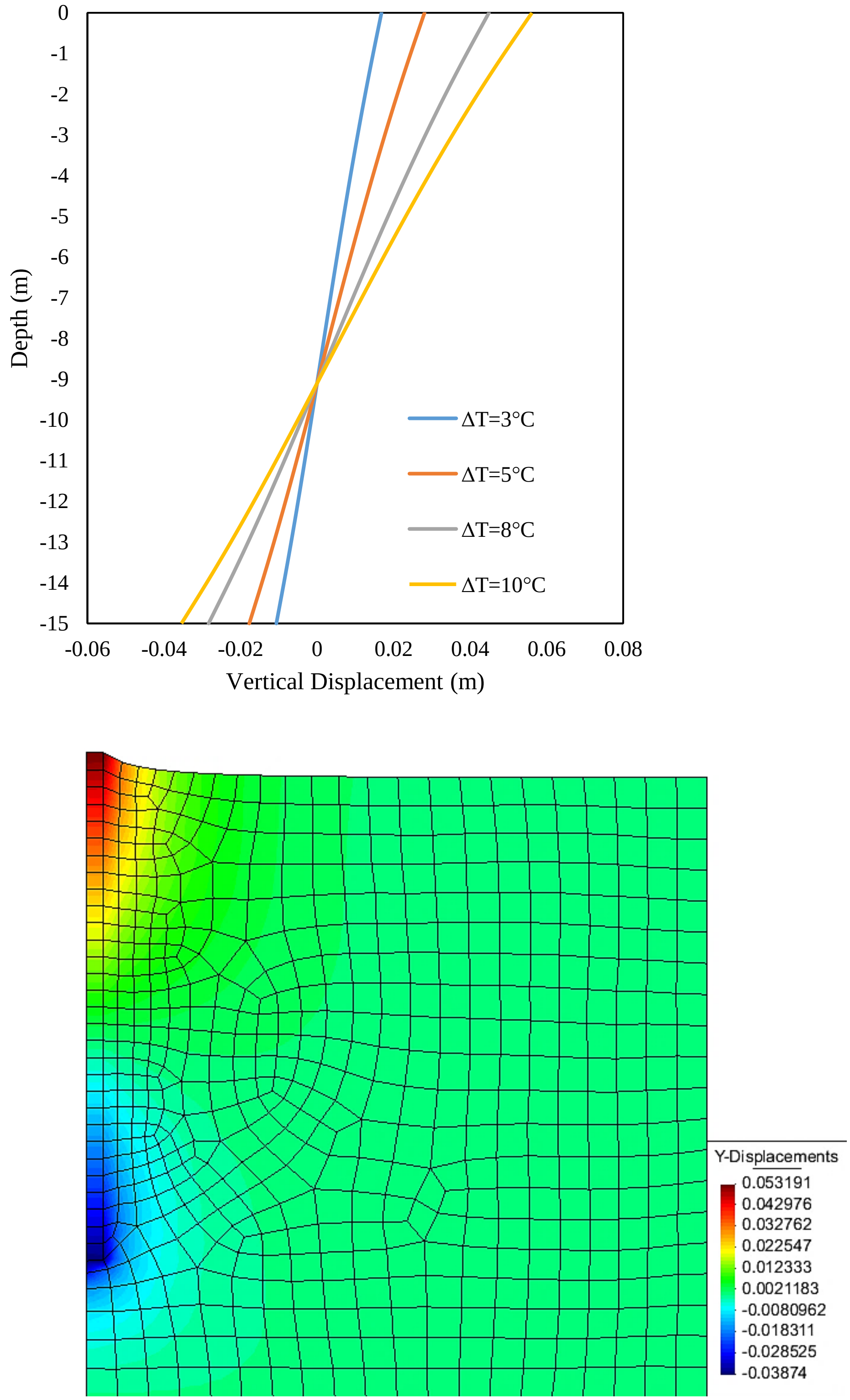

Figure 3- 8: Vertical displacement variation on soil-pile interface with temperature variation

2. Vertical Stress Distribution

Figure 3-9 shows the vertical stress distribution in pile under thermal loading. Under the increased temperature, a pile with free boundary conditions expands. Whenever the pile is constrained, deformations on the pile are prevented, which causes thermal stress in the pile. The stress, which is compressive in nature, is maximum around the mid length of the pile where the expansion was observed to be reversed from upward to downward expansion. The stress value is increasing with a rise in the temperature in the pile. The thermal stress distribution would be symmetrical if the pile was set to be free at both end, but the pile expansion is resisted by soil underneath so the neutral point shifts from mid-point of pile to some downward.

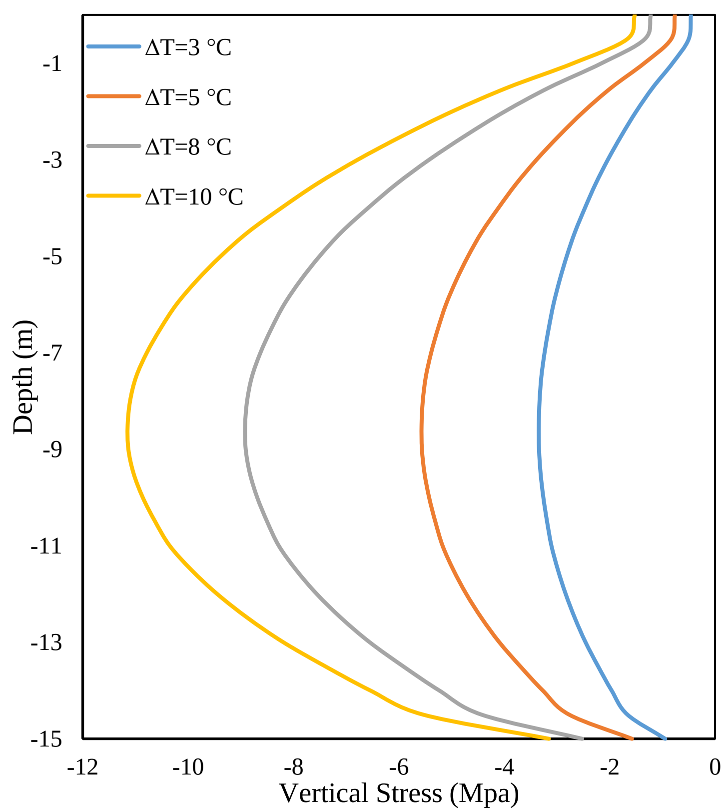

Figure 3- 9: Vertical stress along the soil-pile interface with temperature variation

3. **Shear stress distribution**

The shear stress produced on the soil pile interface during the temperature increment on the pile is shown in the figure 3-10. Because of the heating of the pile, the pile goes on expansion both on the top and bottom of the pile but in opposite direction as shown in the vertical displacement distribution. The shear stress distribution occurs maximum at the ends where the vertical displacement occurs maximum but in opposite direction of the shear stress. At the point of maximum shear stress, the compressive stress becomes minimum and vice versa.

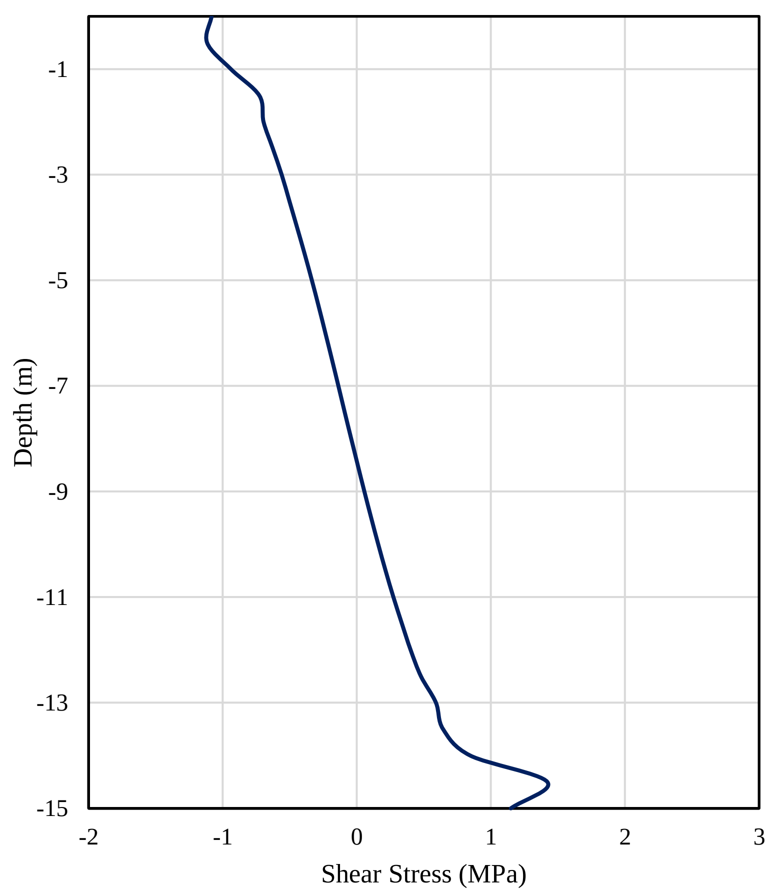

Figure 3- 10: Shear stress distribution on the soil-pile interface in thermal loading

3.3.3 Thermomechanical Loading

Both mechanical load and thermal load were applied on the pile during the thermomechanical simulation of the pile. The initial temperature on the pile and soil was maintained constant (and equal), then the pile was uniformly heated to a certain temperature. Some axial load was applied on the pile head which can be considered as the load transferring from the building to the ground through the pile.

1. Vertical Displacement

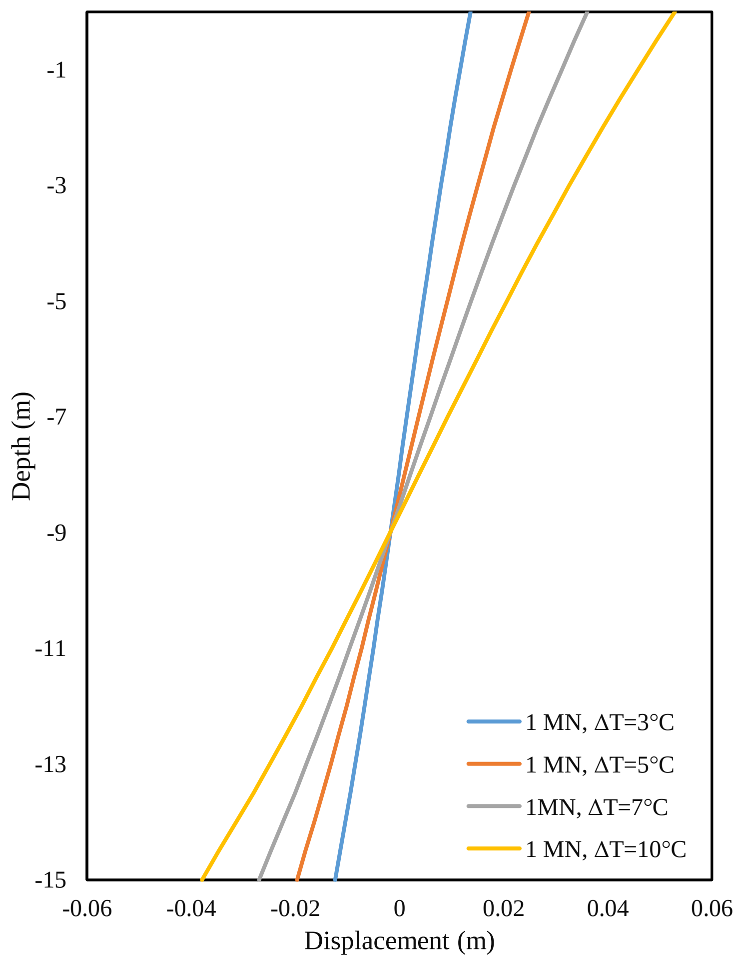

Figure 3- 11: Vertical displacement distribution in the soil-pile interface in thermo-mechanical loading

Figure 3-11 presents the vertical displacement distribution during the thermo-mechanical loading of a pile. Similar to thermal loading, the top part of pile expands upward and bottom part expands downward with changing direction around the midpoint of the pile. The neutral point during the upward and downward expansion is at 8.67 m from the top of pile at $\Delta T=10°C$ and 1 MP loading on the pile foundation. The positive expansion was found to be constrained in the application of mechanical load on the pile. As compared to thermal expansion, it has been constrained to 0.004 m on the same temperature increment with the application of 1MN load.

2. Vertical Stress Distribution

Fig. 3-12 shows the stress variation in pile in three different conditions of loading i.e. mechanical loading (M), thermal loading (T) and thermomechanical loading (TM). In this simulation, the pile was heated by 10 °C in an uniform rate and an external mechanical load of 1000 KN was applied to observe the vertical (Compressive) stress developed in the soil pile interface during thermal, mechanical and thermo-mechanical loadings. From the result of vertical stress distribution in the pile under different loading conditions, it can be observed that the stress due to mechanical loading is in larger quantity at the top of pile which goes on decreasing towards the bottom of pile. The bottom of pile carries almost no stress on it. But in case of thermal loading the stress on the top is smaller than the mechanical loading but the toe of pile is more stressed as compared to mechanical loading. Since the pile is somewhat constrained with soil at the bottom, the curve of thermal loading is not symmetrical about the mid-point of pile. The point of maximum stress would have been at the mid length of pile if it was set free to expand both in top and bottom.

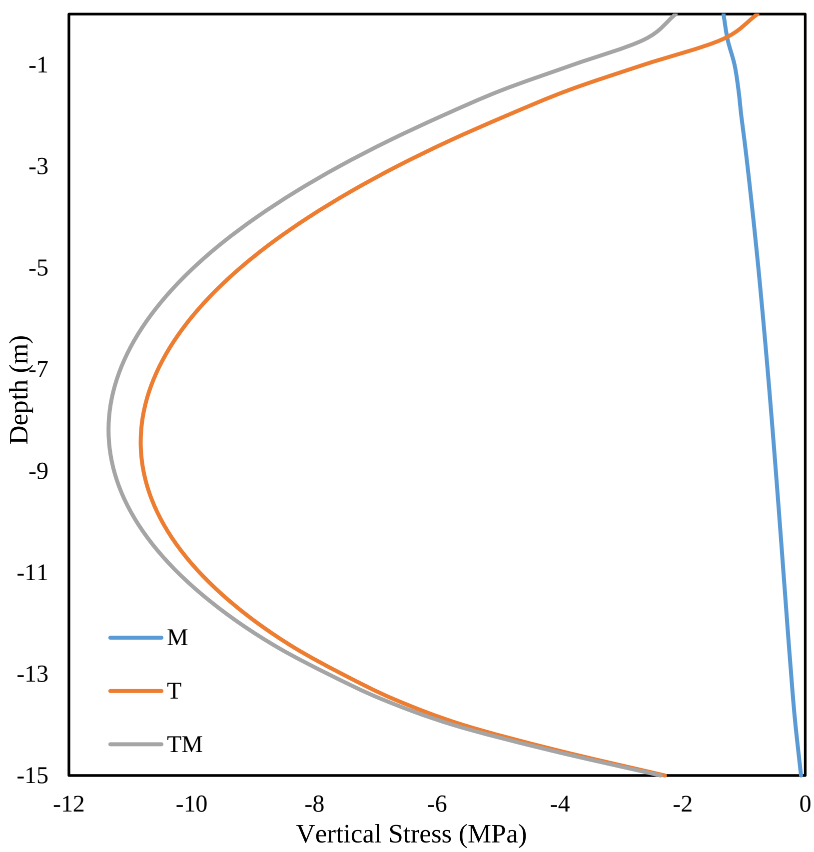

Figure 3- 12: Comparison of vertical stress on the soil-pile interface during mechanical, thermal and thermo-mechanical loadings

The point of maximum resistance shifts from the mid length to some downwards because of the shear resistance and friction provided by soil and the soil pile interface. Ideally the effect of thermomechanical loading should be a combined effect of thermal and mechanical loading which can be observed in almost every part of the pile except in the pile head. At some distance from the top of pile, some “anomalous” distribution of stress can be observed in thermomechanical loading of the pile, which is similar with the results presented in Laloui et. al. 2006. This is possibly due to the fact that the expansion of pile lifts it above the soil and therefore it loses the friction from the soil (hence resulting in the almost constant vertical stress near the top as shown in Figs. 3-9 and 3-12).

3. Shear Stress Distribution

The shear stress distribution during the thermal, mechanical and thermo-mechanical loading is shown in Figure 3-13. On the application of pure mechanical load, the shear stress is maximum at the top of pile and remains almost zero with the depth of pile because during the mechanical loading all the force applied from the top of the pile transferred to the bottom without causing a lot of friction. But during the thermal load application the pile goes on thermal friction with the scenario of upward and downward expansion so the shear stress variation changes from negative to positive with the depth of the pile as in the figure for shear stress distribution.

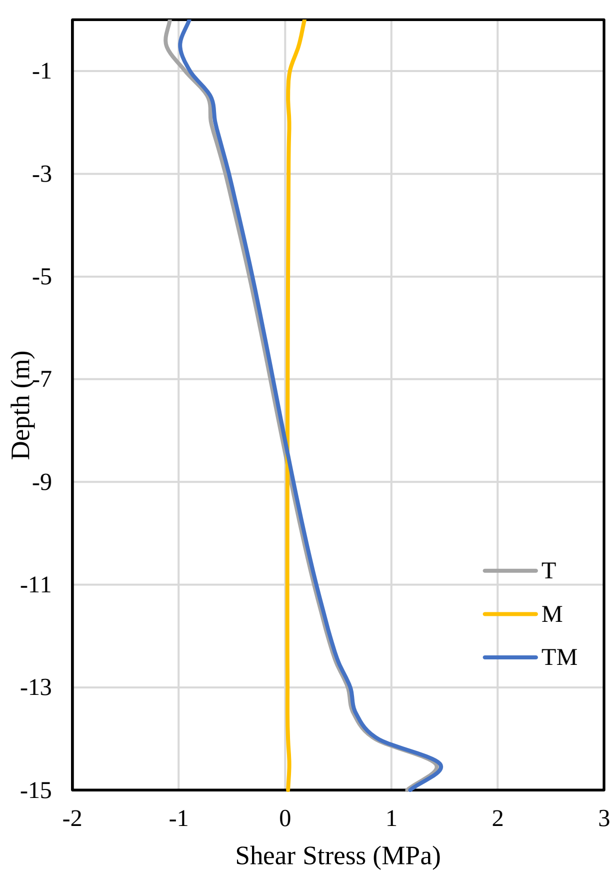

Figure 3- 13: Comparison of shear stress on the soil-pile interface during mechanical, thermal and thermo-mechanical loading

3.4 Influencing Distance

In this section, we also investigated the deformation and stress in the surrounding soil, in particular, the distance up to which the soil is significantly affected by the heating/cooling of the pile, referred to as influencing distance of the load. Stress, strain and displacement in vertical and in horizontal direction from the soil pile interface are presented in the following section of this chapter. Figures 3-14 and 3-15 can be used to assess the influencing distance from the soil pile interface in case of thermal and thermomechanical loading. In both the thermal and thermomechanical loading, vertical stress variation is maximum at the soil pile interface which gradually decreases away from the interface. The vertical (compressive) stress tends to zero value at a distance of 0.4m from the pile. Moreover, the stress variation is irregular at a distance from soil pile interface as compared to that at soil pile interface. At 0.4 m from the interface, some mid-length portion of soil encounter negligible stress value as compared with other values. It is therefore reasonable to qualify this distance, 0.4m from the soil pile interface, as the maximum influencing distance, which is valid both in thermo-mechanical loading.

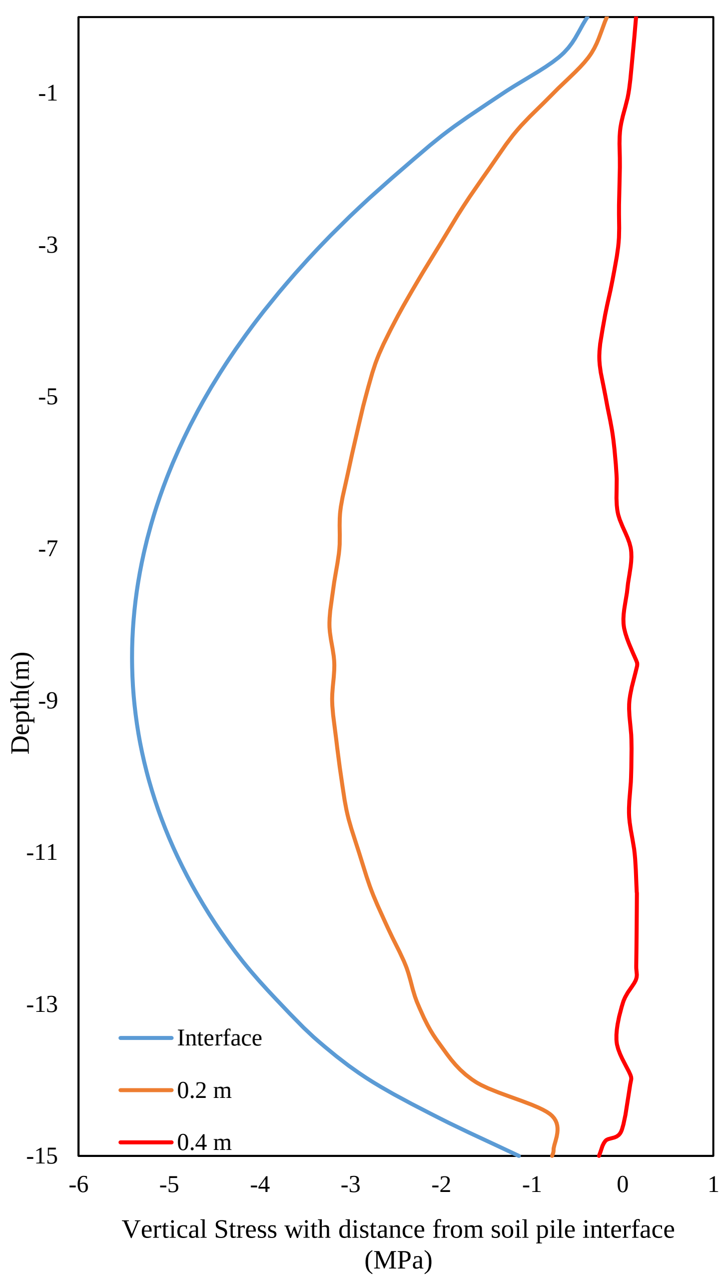

Figure 3- 14: Vertical stress variation at the soil-pile interface and at 0.2 m and 0.4 m away from the interface on thermal loading

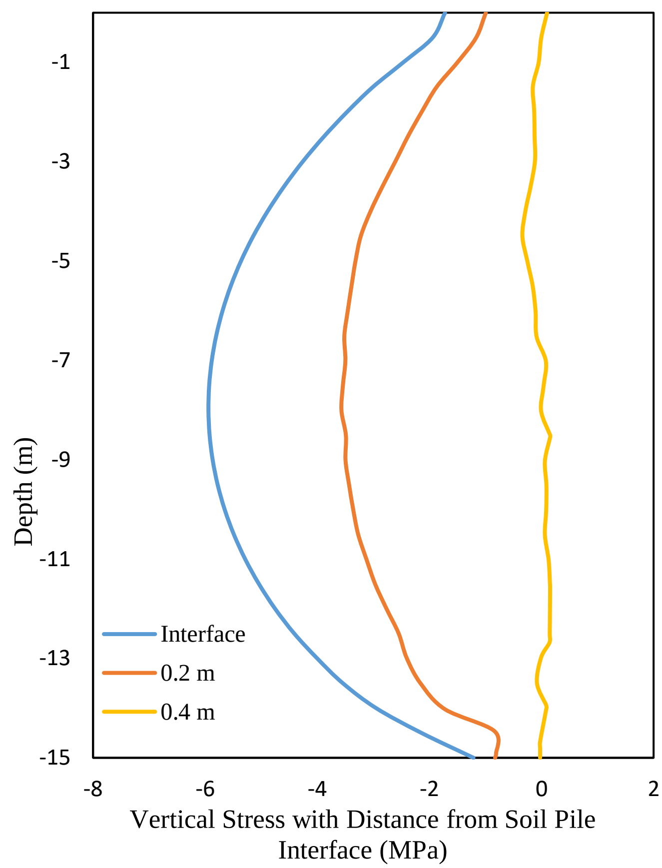

Figure 3- 15: Vertical stress variation at the soil-pile interface and at 0.2 m and 0.4 m away from the interface on thermo-mechanical loading

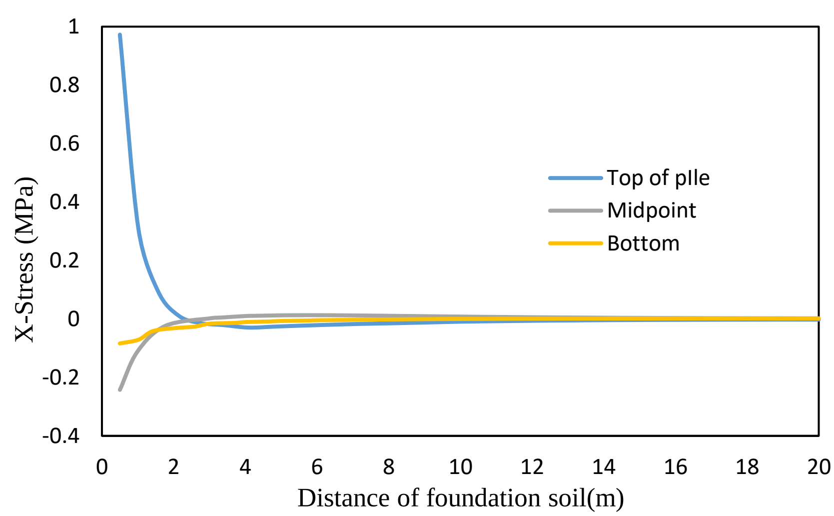

Figure 3- 16: Horizontal stress variation in foundation soil due to thermomechanical loading

Fig. 3-16 presents the stress variation in horizontal direction in soil deposit away from the center of the pile. The horizontal stress decreases in a certain distance after which the variation becomes negligible. The horizontal stress was checked at three different depths of the pile, one at the top, at the middle of pile and at the bottom of the pile. It can be observed that the horizontal stress is maximum at the top of pile which decrease up to 3 m from the center of pile, beyond that the horizontal stress on the soil is negligible. Moving from top to bottom of the pile, the horizontal stress becomes compressive and becomes negligible at the pile toe. In each case, either top, middle or bottom of pile the horizontal stress is negligible beyond 3m from the pile center or 2.5m from the soil pile interface. If we consider different value of mechanical and thermal loading along with the properties of soil and pile during the simulation, the value of stress may be different as compared to the values calculated in this paper but the influencing distance is somehow similar in every case.

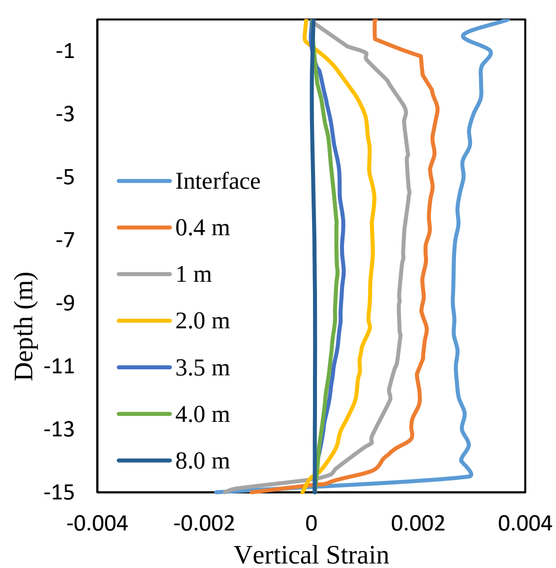

Figure 3- 17: Vertical strain variation at the soil-pile interface and on the soil up to 8 m from the interface

The vertical strain produced by the thermomechanical loading is maximum at the top of pile at the soil pile interface which remains almost similar throughout the pile depth as shown in Figure 3-17**.** At the toe, the strain value is almost zero and changes from positive to negative towards the soil deposit underneath the pile. The effect of loading on strain can be seen clearly up to a distance of 0.4 m from the pile. Beyond 0.4 m, strain at the top and bottom of pile are negligible but the middle portion have very small strain which goes on reducing as we move further away from the pile. Beyond 0.4 m the strain is negligible at top and bottom but remains maximum at the mid length of pile where the stress is maximum.

3.5 Summary

This chapter presents the analysis of thermomechanical loading on a pile foundation where a numerical model of a heat exchanger pile was analyzed in stationary and symmetric condition. A mechanical load was applied to the top of the pile while the thermal load was applied in uniform increment of temperature in the pile surface. The behavior of pile under these loadings was analyzed with reference to stress, strain and displacement occurred in the pile in different conditions of loading. Under mechanical loading only, the stress is maximum at the pile head and decreases towards the toe. In the presented simulation, the load is primarily transferred to the surrounding soil via friction, hence the stress at the bottom of the pile is very small. Under a heating scenario of temperature rise in the pile but in the absence of mechanical loads, it was found that the pile was expanded in both the upward and downward direction in the value equivalent to the manual calculation too. The vertical compressive stress was found to be minimum at the top and bottom of the pile with maximum stress concentration about the mid depth of the pile. Under the combined effects of mechanical and thermal loading, the compressive vertical stress in the pile reaches maximum near the mid-length of pile, but due to the constraint/reaction from the soil at the bottom, the maximum value of shear stress occurs at some distance slightly below the mid length of pile. The point of maximum stress is also called the point of inversion or null point because the vertical displacement and shear force changes from positive to negative from this point. The results also show that in a thermal-elastic analysis, the results can be approximately achieved via a superposition of mechanical loading and thermal loading.

The influencing distance due to thermomechanical loading on the pile was studied in this chapter. While simulating the model for these analyses the soil with normal stiffness was considered. The vertical stress produced in soil because of thermal and thermomechanical loading is dominant in the soil pile interface which tends to be zero within 0.4 m from the pile. While analyzing the horizontal stress, the maximum influencing distance is within 3 m from the pile similar is the case in strain observation too. From these studies the influencing distance can be considered as 3 m from the soil pile interface for thermal and thermo-mechanical loading.

Chapter 4

Influence of Surrounding Soil Undergoing Coupled Thermo-Hydro-Mechanical (THM) Processes

4.1 Introduction

In the preceding section, efforts are primarily devoted to the thermo-mechanical behavior of the heat exchanger pile, the surrounding soil is modeled as a classical continuum without consideration of the presence of pore water, i.e., a dry material whose deformation is governed by its total stress; this approach also echoes a typical methodology adopted in the majority of the numerical investigations in the existing literature reviewed in Chapter 2. However, in classical soil mechanics the presence of water phase in soil voids renders an effective stress approach necessary to describe the mechanical behavior of the soil, and conventional design of pile foundation also depends on the effective strength parameters. It is of great interest to examine the behavior of heat exchange piles surrounded by soils which experiences typical hydraulic scenarios. In addition, a preliminary investigation on the possibility of coupling of different thermal and hydraulic processes in partially saturated soils undergoing wetting or drying cycles is also explored in the chapter.

Three cases are examined in this chapter. In the first two scenarios, the surrounding soil was saturated, whereas in the third scenario an attempt to explore the effect of partially saturated soil on the performance of heat exchanger pile has been carried out. The geometric configuration including the kinematic boundary conditions is identical to the investigation presented in Chapter 3 (Fig. 3-1). Due to the involvement of hydraulic flow, the modeling of soil behavior entails a thermo-hydro-mechanical character. Therefore, the modeling presented in this chapter is hereafter referred to as THM modeling, in contrast to thermo-mechanical (TM) analysis discussed in the preceding chapter.

4.2 Scenario 1:Constant Mechanical Loading and Varying Temperature Change in the Pile Surrounded by Saturated Soil

In this scenario, a constant mechanical load was applied to the top of the heat exchange pile, where the mechanical load on the pile was kept constant at 1000 KN and water pressure was applied linearly from zero on the top of the soil deposit to maximum i.e., water pressure equivalent to 20 m depth, at the bottom as shown in the loading diagram as shown in Figure 4-1.

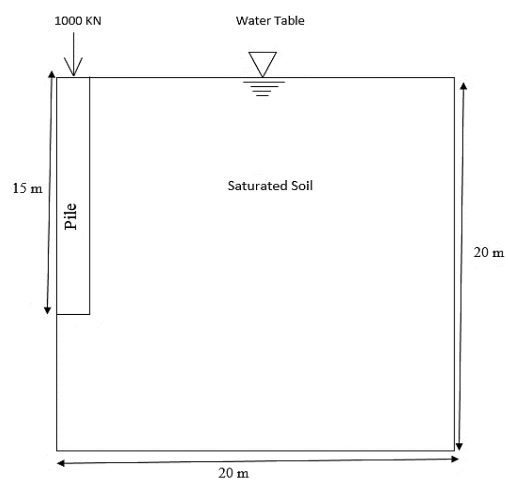

Figure 4- 1: A schematic representation of the simulated domain consisting of the pile under a constant load of 1 MN and the surrounding saturated soil

4.2.1 Response of the Heat Exchanger Pile

The vertical displacement on the soil pile interaction at constant load with variation in temperature is shown in Figure 4-2. The upward expansion from the middle of pile is more than the downward expansion, in other words the upward and downward expansion are not symmetrical to each other. The neutral point or the point of inversion can be found at 8.72 m depth from the top of pile at ΔT = 10°C temperature and 1000 KN load which is 0.05m below the neutral point obtained during the TM loading. Because of the water pressure it can be observed that the total displacement in the pile increased as compared to the TM loading because the static water pressure acts as a superimposition to the mechanical loading besides the hydraulic scenario.

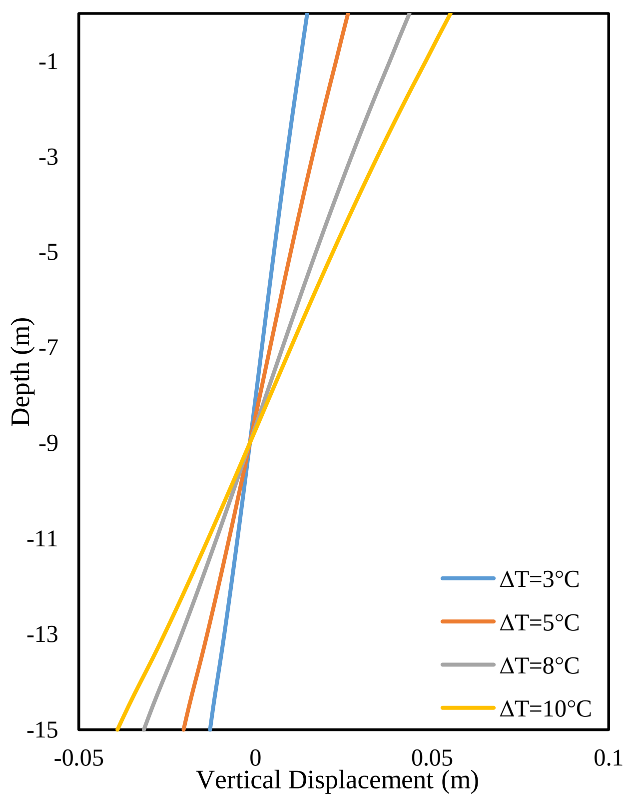

Figure 4- 2: Vertical displacement in the soil-pile interface under constant mechanical loading on

During the THM simulation with external mechanical load on the pile, with the increase in temperature and water pressure, the stress variation is similar with the thermo-mechanical loading as shown in Figure 4-3. The maximum stress obtained during THM simulation is in between 8.5 m and 9 m depth in different temperature increments while during TM loading the maximum stress was in between 8 m and 8.5 m depth from the top of pile. At about 1 m depth, there is some deviation in the stress diagram as compared to TM loading, which may be the cause of water pressure on the pile.

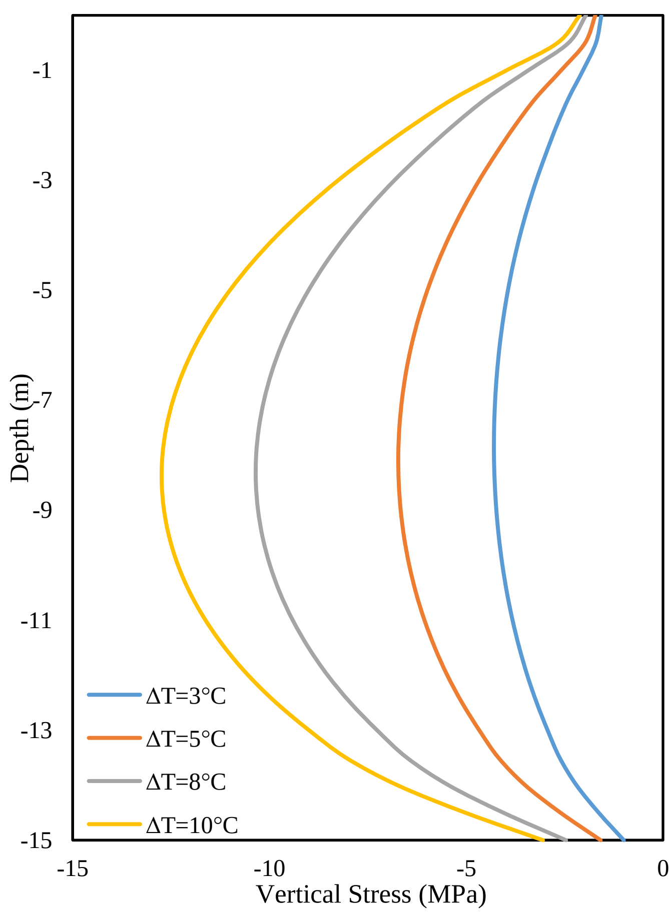

Figure 4- 3: Vertical stress distribution on the soil-pile interface under constant mechanical loading with varying temperature

4.2.2 Response of Surrounding Soil

The vertical strain distribution in the soil pile interface in different temperature distribution under the THM loading is presented in Figure 4-4. From the figure, it can be observed that, the strain is maximum around the pile head whereas it goes slightly negative around the toe.

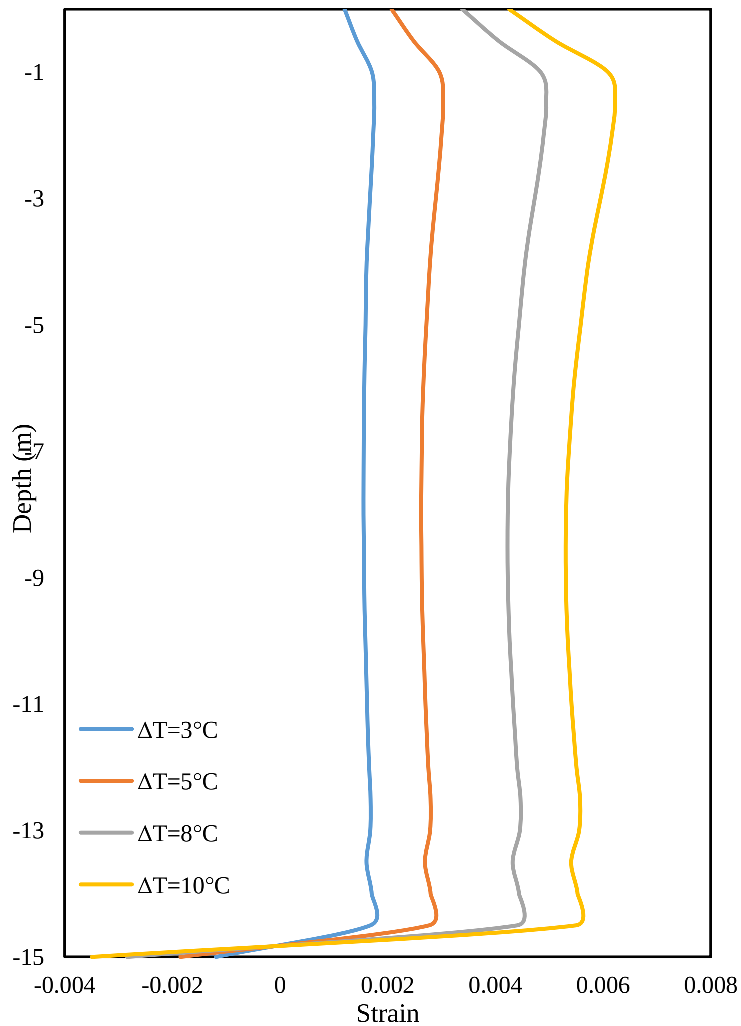

Figure 4- 4: Vertical strain distribution at the soil pile interface under constant mechanical loading and varying temperature

The strain is almost constant throughout the pile but it goes increasing towards the pile head in the THM modeling. During TM simulation, the strain variation was symmetrical around the pile depth with maximum strain at the mid pile depth and minimum (almost zero) at pile edges.

The comparison of total stress with the effective stress during the saturated condition of soil with TM loadings is shown in Figure 4-5. From the figure, the effective stress is equal to the total stress at the top of the soil where the liquid pressure is zero.

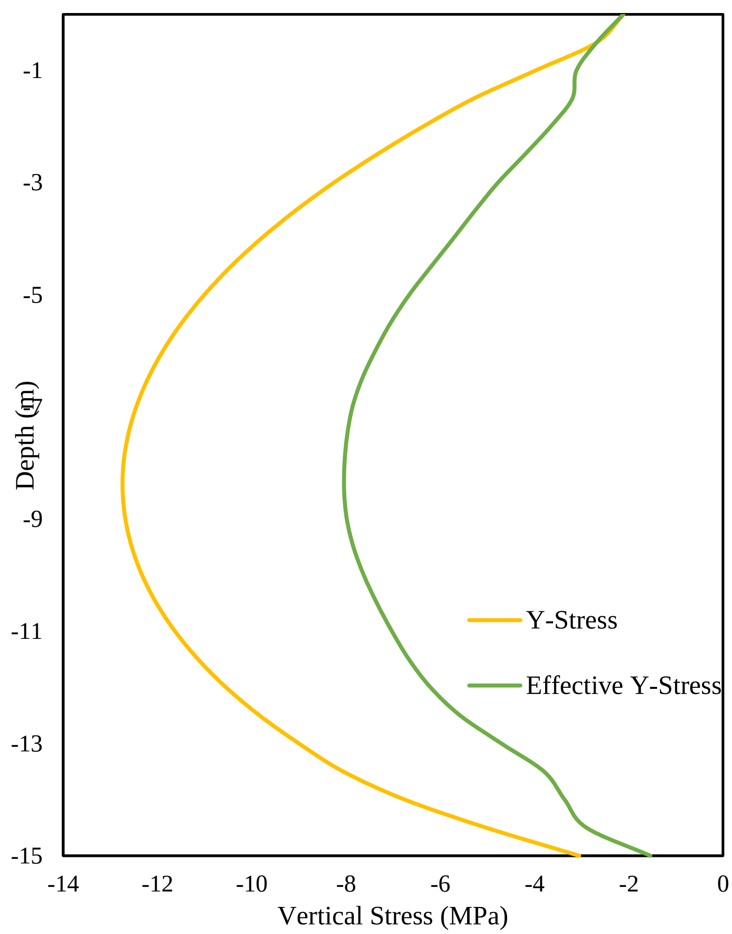

Figure 4- 5: Comparison of total stress with effective stress at the soil-pile interface in saturated soil with 1000 KN of mechanical load and ΔT=10°C

4.3 Scenario 2: Constant Temperature and Varying Mechanical Load on the Pile Surrounded by Saturated Soil

On another part of simulation, the temperature increment on the pile was kept constant and the model was simulated for different mechanical loading to observe the mechanical behavior of pile. The results obtained from THM simulation with constant temperature are presented in the following section.

In this section part of analysis, the pile was heated by a constant temperature, i.e., 10°C in this simulation, and the mechanical load on the pile was varied to observe the effect of load variation with a constant temperature and saturated soil. The vertical stress, vertical strain and vertical displacement were observed and the results are presented in the following section.

4.3.1 Response of the Heat Exchanger Pile

During the THM analysis under constant temperature and variable mechanical loading, the obtained result for vertical displacement is shown in Figure 4-6. It can be seen that a similar nature of curve for all the values of mechanical loading from very small load to a higher load. Similar to the TM loading the null point lies somewhere between 8.5 m and 9 m, but the upward and downward expansion nature of the pile are different in this simulation. The change in displacement from one load to other is very minimal though the load has been increased in a large amount. From the figure, with the increase mechanical loading, the displacement or upward expansion value has been decreased with some value whereas there is increment in the downward expansion value. The effect of mechanical loading was found to be too small under the constant temperature as compared to the thermal loading in the vertical displacement of pile. In this case, with the increase in mechanical loading the upward expansion was found to be decreasing which is because the loading acts as a mechanical with temperature effect on it. Since on the simulation with mechanical loadings only, the vertical displacement was found to be more compressive with the addition of more external loads on the pile the same scenario acts in this case of loading too.

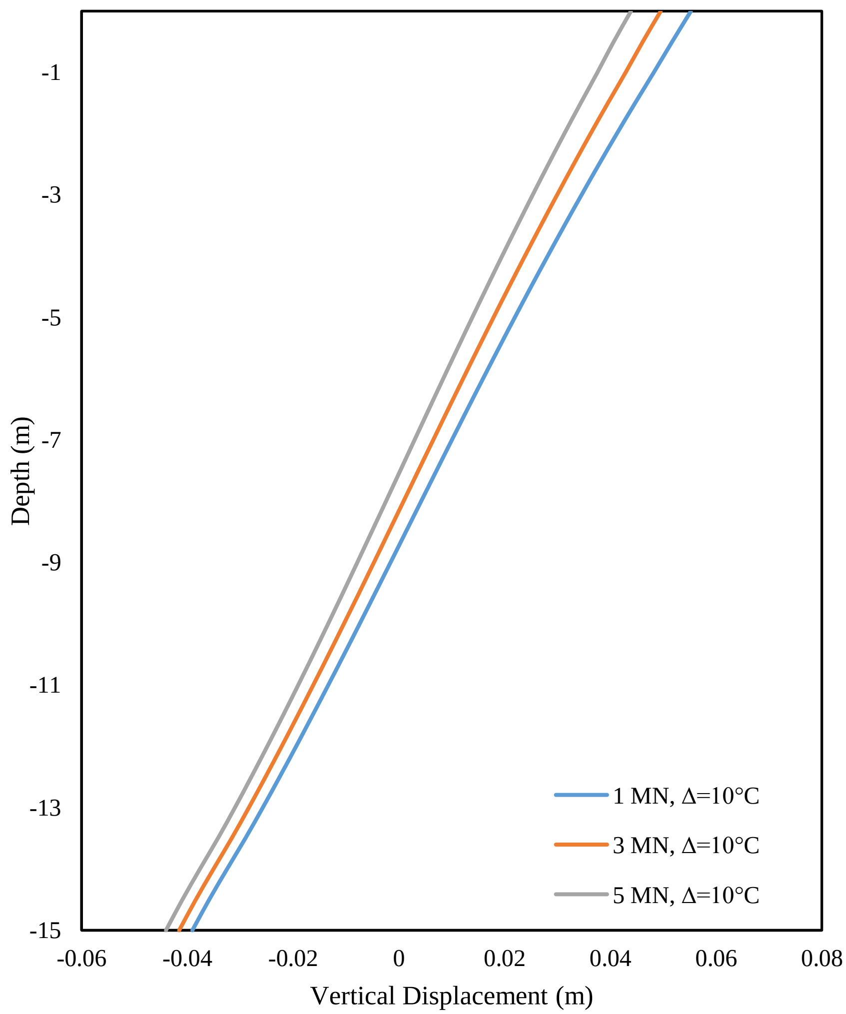

Figure 4- 6: Vertical displacement distribution at the soil-pile interface under constant temperature ($\Delta T=10^0$ C) and varying mechanical loads on the pile axis

The vertical stress distribution under THM loading with constant temperature increment and with the increment in mechanical loading can be seen in Figure 4-7. The graph of the vertical stress is more comparable with the stress distribution during the thermo-mechanical loading with the effect of heating on the pile.

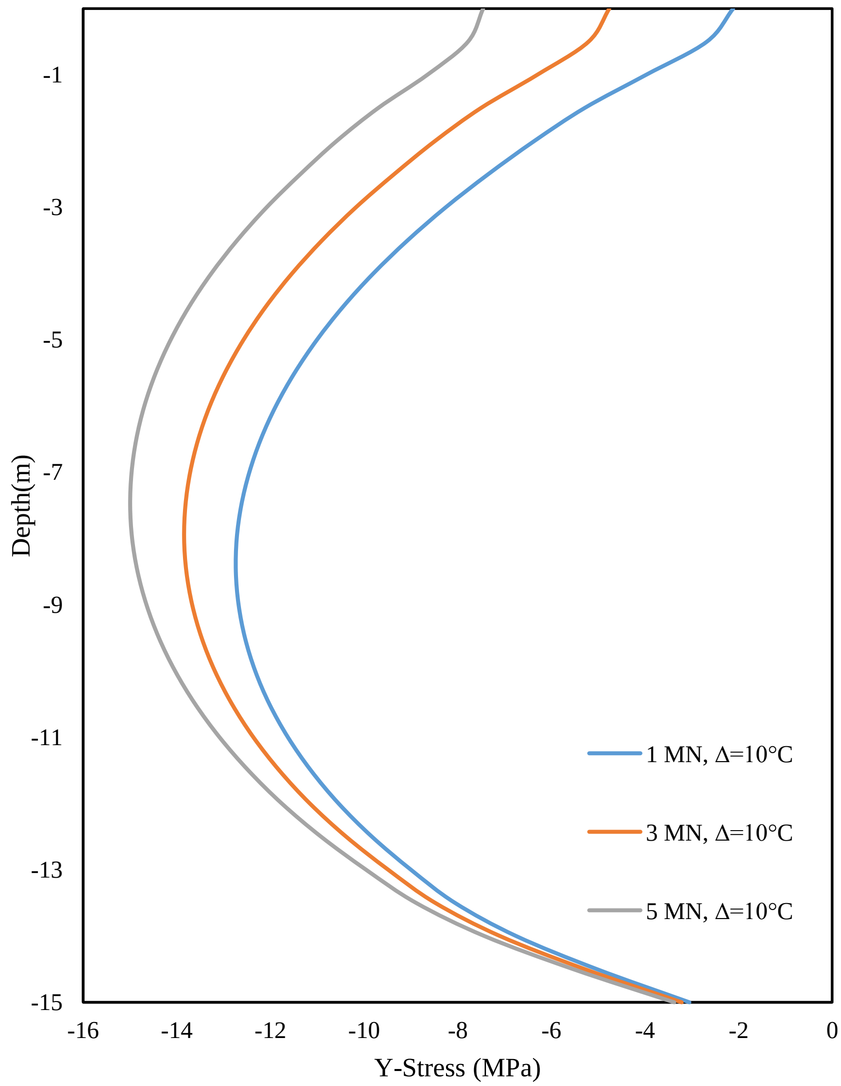

Figure 4- 7: Vertical stress distribution at the soil-pile interface during constant temperature (ΔT=10^0 C) and varying mechanical load on the pile axis

The strain distribution in the pile during the THM simulation with temperature being constant and increment in the mechanical load is shown in Figure 4-8. The strain variation curve depicts that the positive strain on the top of pile goes on decreasing with the increase in mechanical load whereas the negative strain at the bottom of pile increases with such loading.

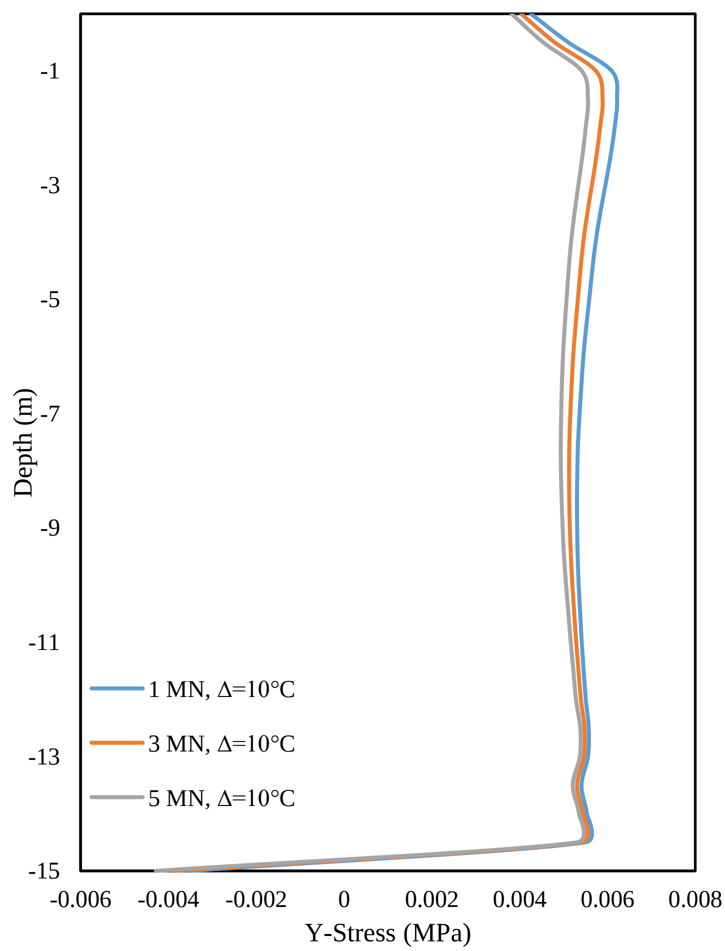

Figure 4- 8: Vertical strain distribution under constant temperature ($\Delta T=10^0$ C) at the soil-pile interface with varying mechanical load on the pile axis

4.3.2 Response of surrounding soil and a comparison of results for TM and saturated THM condition

The mechanical properties of the pile at the soil-pile interface during the thermo-mechanical and thermo-hydro-mechanical condition of loading were compared and are analyzed in this section. The figure shows that the vertical displacement, vertical strain, the vertical stress as well as shear stress increases during the simulation with fully saturated condition of soil because the applied static liquid pressure on the foundation soil also acts as a part of mechanical load besides the hydraulic loading scenario.

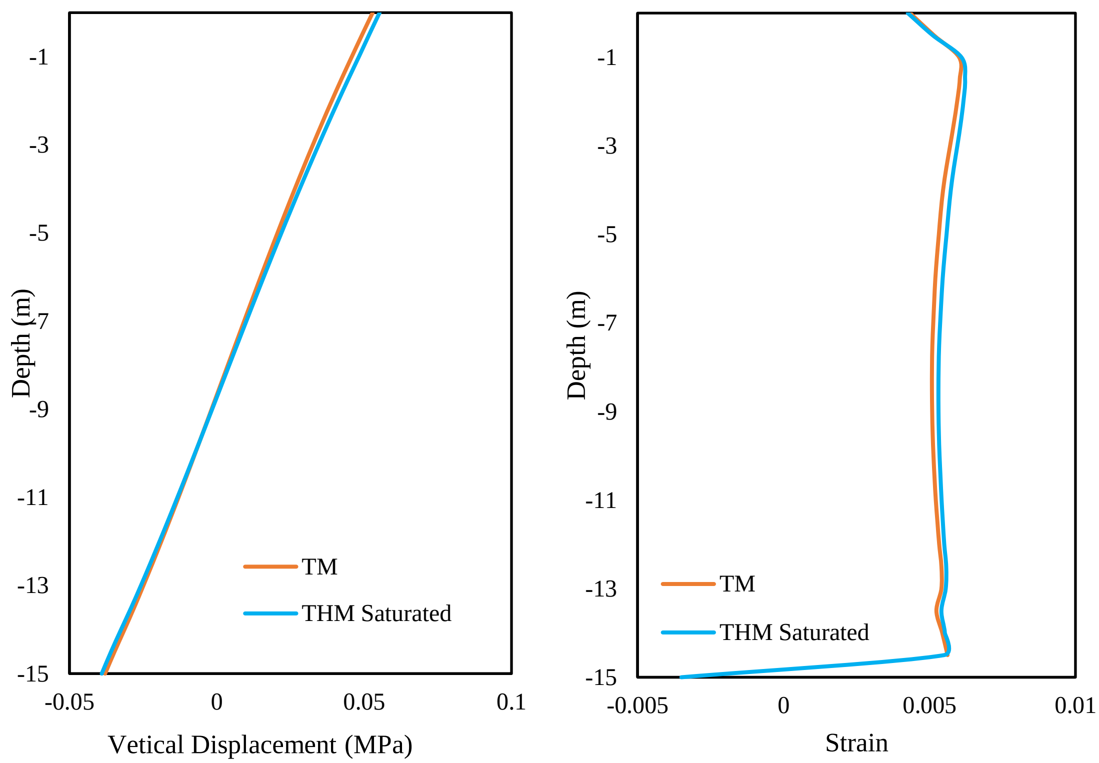

Figure 4- 9: Comparison of vertical displacement and vertical strain at the soil-pile interface during TM and saturated THM loading condition

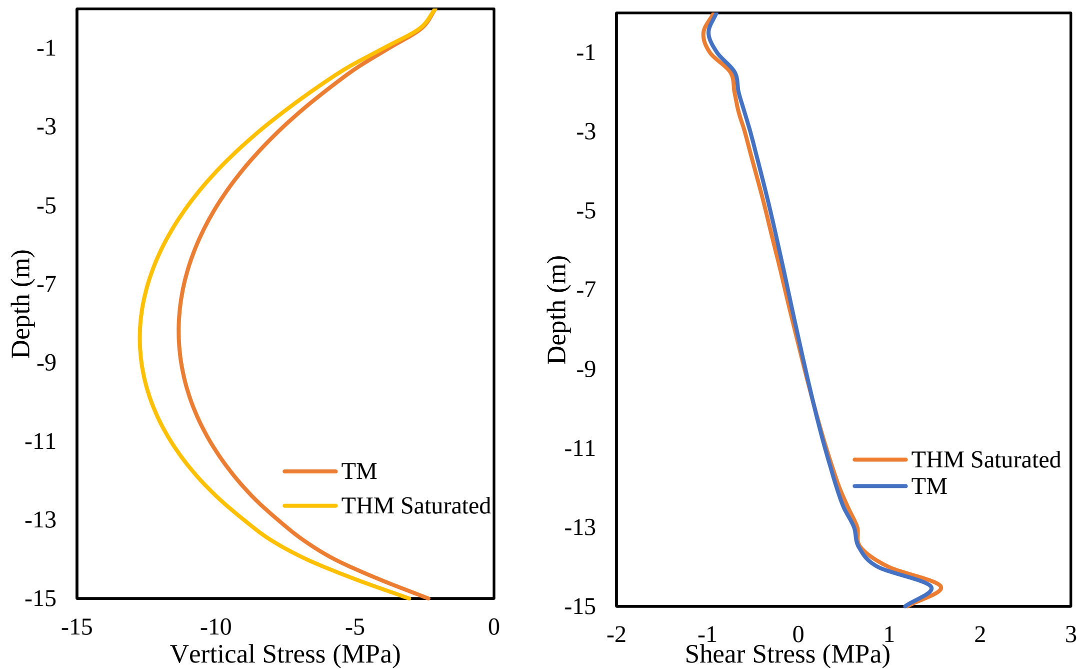

Figure 4- 10: Comparison of vertical stress and shear stress at the soil-pile interface during TM and saturated THM loading condition

4.4 Scenario 3: A preliminary investigation of the effect of partially saturated soil on the performance of heat exchanger pile

On the second part of the simulation for the analysis of THM loadings, an attempt was made to study the effect of unsaturated condition of hydraulic loading on the performance of heat exchanger pile. The water table was set at 5 m below the top of the soil deposit and increased linearly to the bottom in liquid pressure equivalent to the 15 m of water as presented in Figure 4-11. The responses of the unsaturated soil on the heat exchanger pile are summarized in the following section.

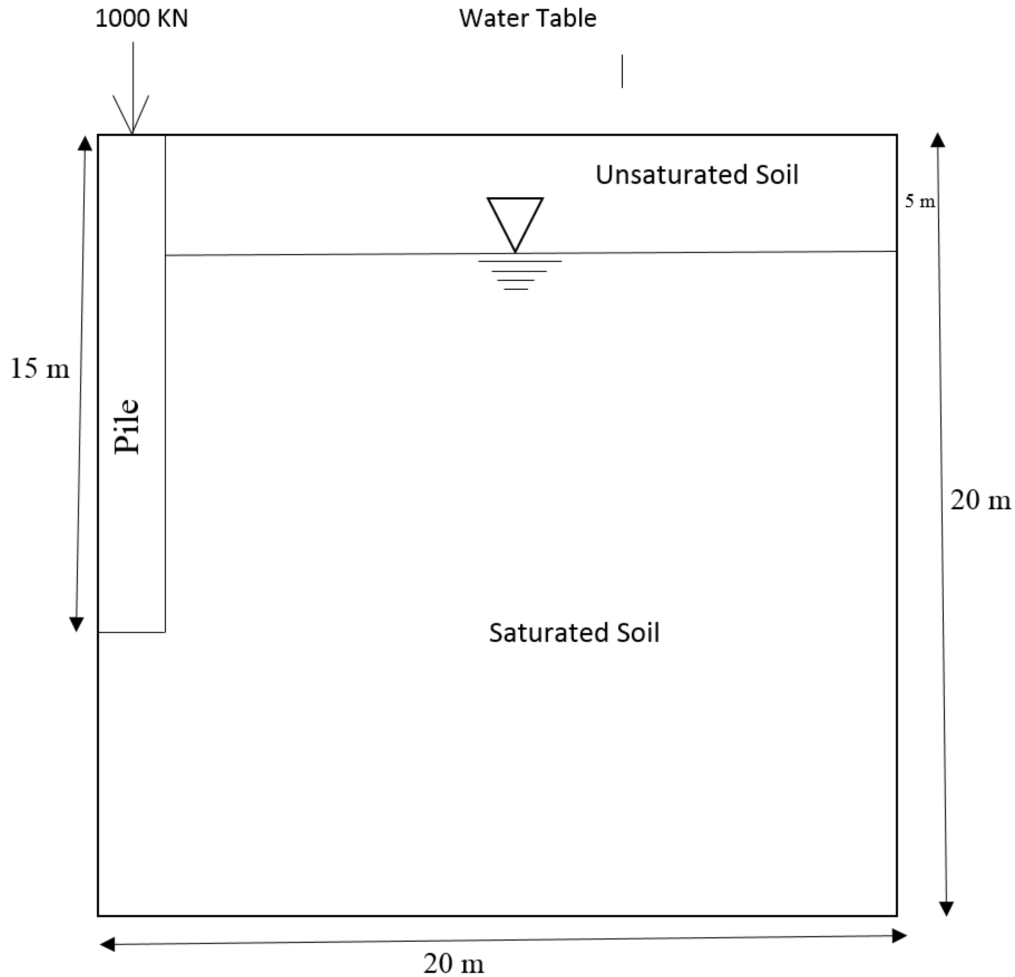

Figure 4- 11: A schematic representation of the simulated domain consisting of the pile under a constant load of 1 MN and the surrounding unsaturated soil

The vertical displacement during the unsaturated simulation of soil is shown in Figure 4-12. As compared to saturated condition, it was found that the unsaturation of soil effects on the vertical displacement, compressive stress as well as the location of neutral point on the heat exchanger pile. The effect of unsaturation on the vertical displacement and vertical stress are shown on Figure 4-12 and 4-13 whereas 4-14 represents the strain on the soil due to loading on the pile with all other conditions of thermal and mechanical loading remaining the same as in the simulation for saturated condition of soil. The effect of unsaturation can be observed in top part of the curve in vertical displacement, vertical compressive stress and strain at the soil-pile interface, where we can observe some irregularity on the curve as compared to saturated condition which may the cause of capillary pressure on the region of unsaturated zone.

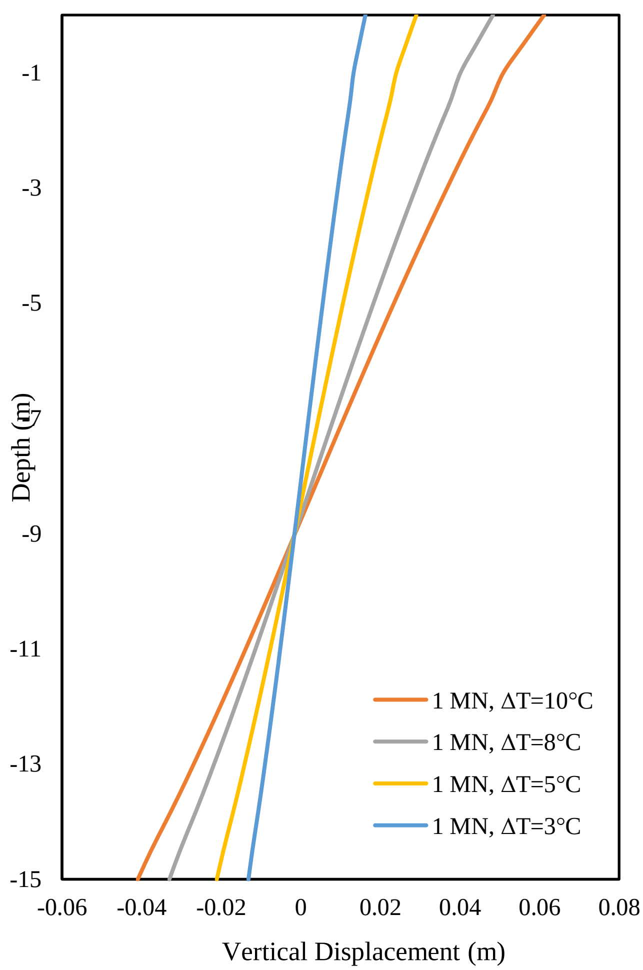

Figure 4- 12: Vertical displacement distribution at the soil-pile interface in unsaturated soil with temperature increment

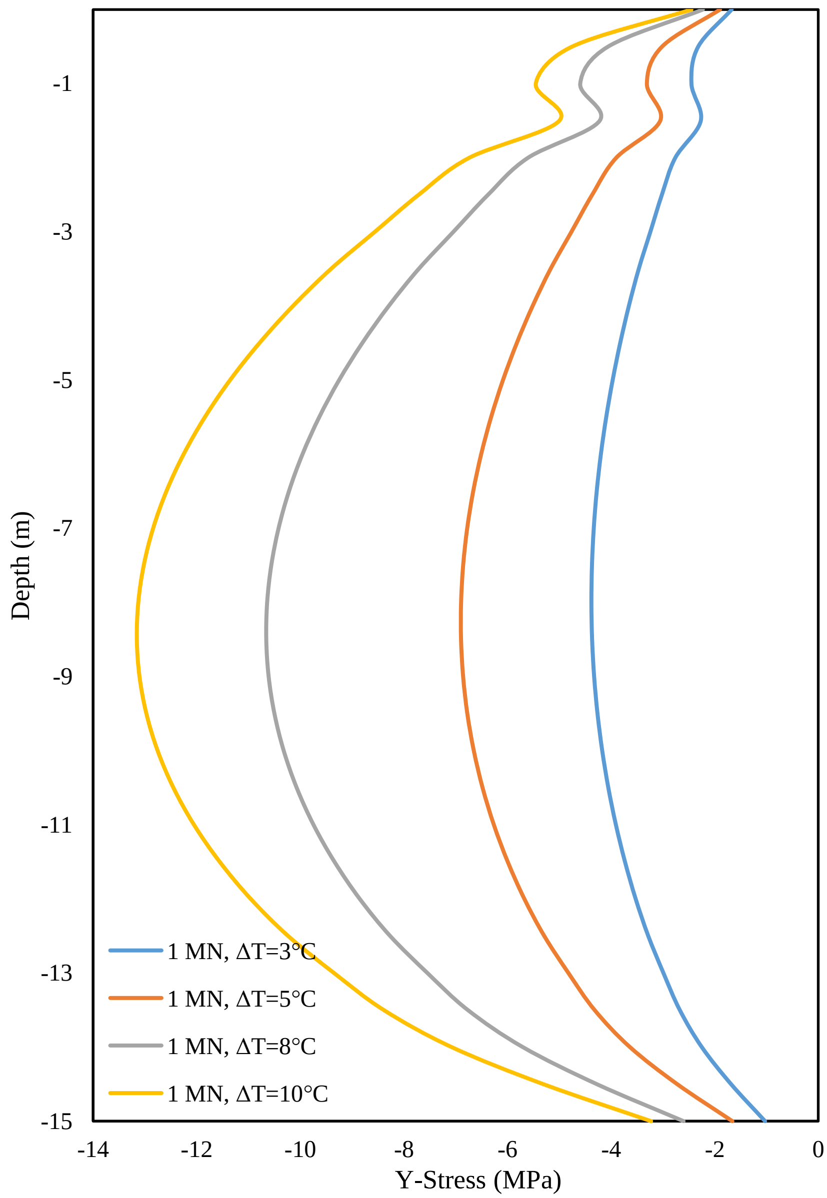

Figure 4- 13: Vertical stress distribution at the soil-pile interface in unsaturated soil with temperature variation

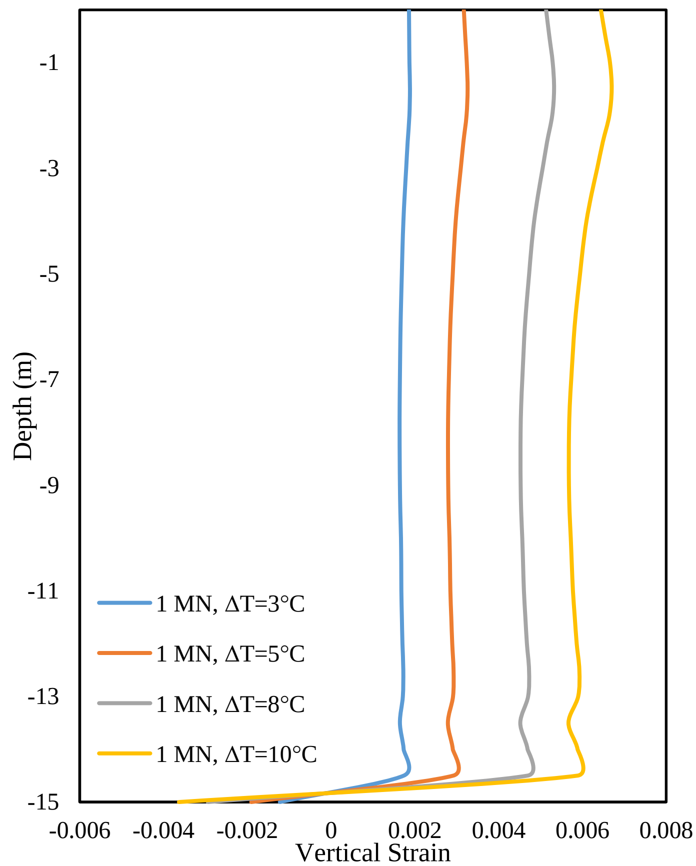

Figure 4- 14: Vertical strain distribution at the soil-pile interface in unsaturated soil with varying temperature

4.5 Influencing Distance

The influencing distance in thermo-hydro-mechanical loadings was determined with the analysis of vertical stress, horizontal stress and vertical strain up to a certain distance from the soil pile interface. A numerical simulation was performed with 1000 KN of external loading and 10°C rise in temperature of the pile with a liquid pressure equivalent to 20 m of soil.

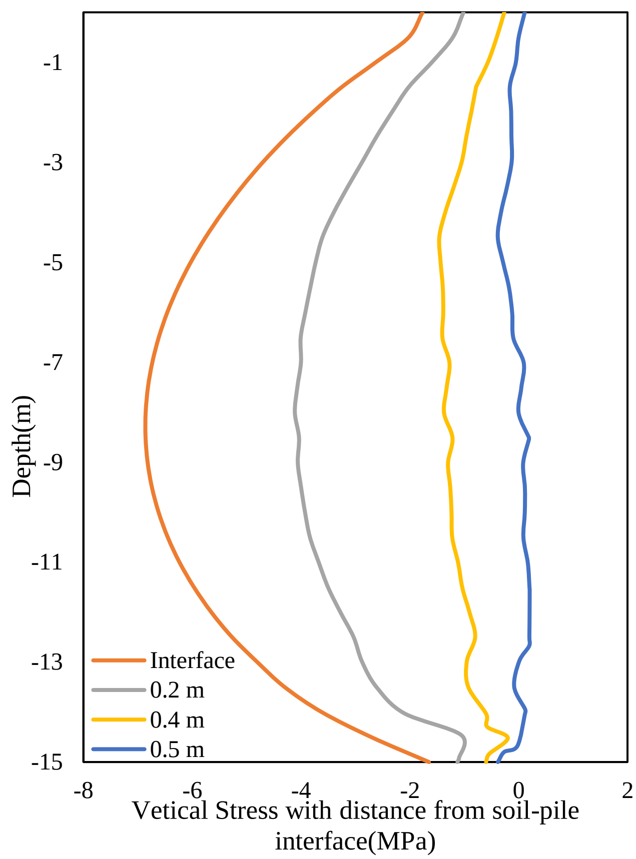

Figure 4- 15: Vertical Stress variation at a with distance from soil pile interface

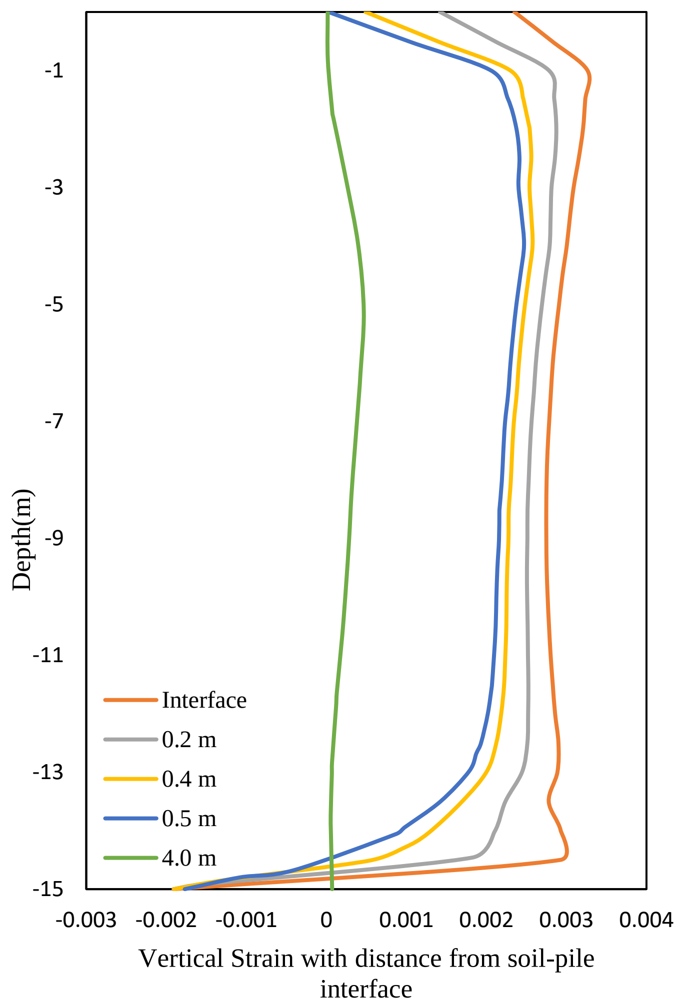

Figure 4- 16: Vertical strain variation with the distance from the soil-pile interface

From the vertical stress and vertical strain analysis from Figs 4-15 and 4-16, it can be considered that the soil within 0.5 m from the soil pile interface can be affected because of thermo-hydro-mechanical loadings. At 0.5 m from the interface, the vertical stress on the soil is almost zero throughout the soil deposit. In the analysis of vertical strain produced by the coupled loading on pile foundation, the strain values are negligible at a distance of 4 m from the interface whereas these values are considerably small at 0.5 m from the soil pile interface.

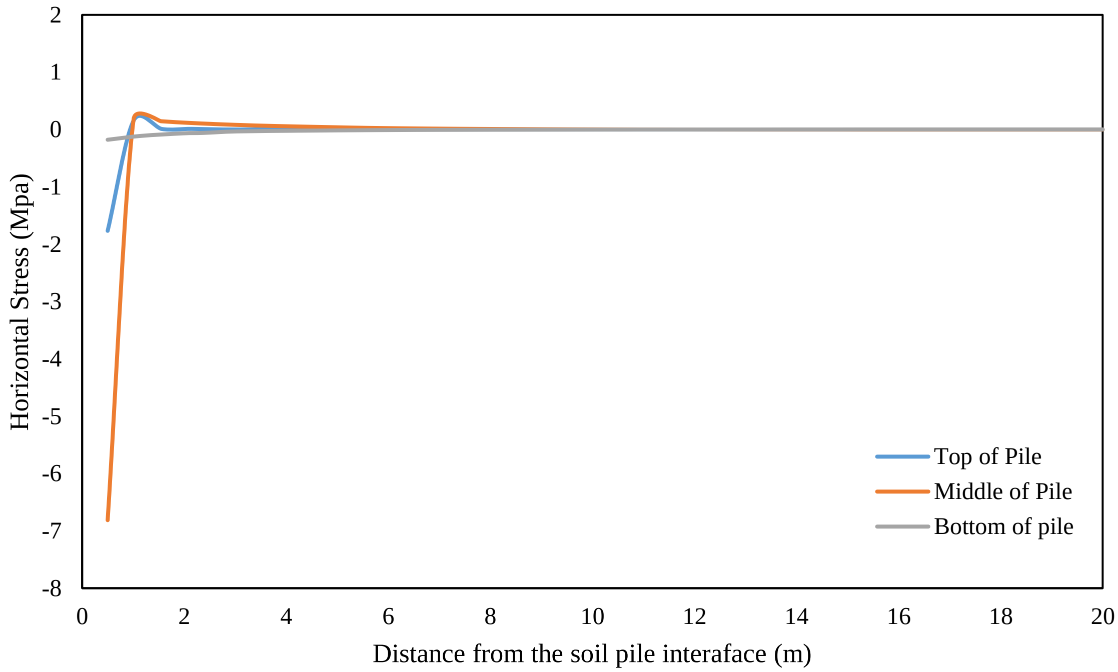

Figure 4- 17: Horizontal stress variation with distance from the soil-pile interface

From the inspection of horizontal stress, Figure 4-17, distribution at top, middle and bottom of the pile, it can be observed that the soil within 4 m can have effect of the loadings. The bottom of the pile doesn't have a major effect on the horizontal stress development on the soil as compared with top and middle portion of the pile. The stress formation is maximum at the middle portion of the pile where the effect of horizontal stress can be noticed up to 4 m from the soil pile interface.

4.6 A Parametric study on the simulation of heat exchanger pile

Different parametric studies were made along with the analysis of mechanical behavior of pile foundation at the soil-pile interface during the different combination of loads applied on the pile foundation. Some of the studies made are presented in the following section:

1. Vertical Stress Development with the Stiffness of Soil

While considering the relationship of mechanical behavior of soil pile interface with the stiffness (strength) of soil under the THM loading, it can be observed a directly proportional nature on the stress development with increase in soil stiffness within 100 MPa. Beyond 100 MPa, the stress is linked with hardness of soil with a curved graph as shown in figure 4-18. The graph shown below shows the relation in the stress development with the nature of soil under similar boundary condition, flux condition with water pressure, temperature increment and mechanical loading. During the initial stiffness increment, there is a rapid increment in the stress e.g. if we increase the stiffness from 100 MPa to 200 MPa, the stress increases by 15 MPa but when the stiffness increases from 500 MPa to 1000 MPa, the stress increases by 12 MPa.

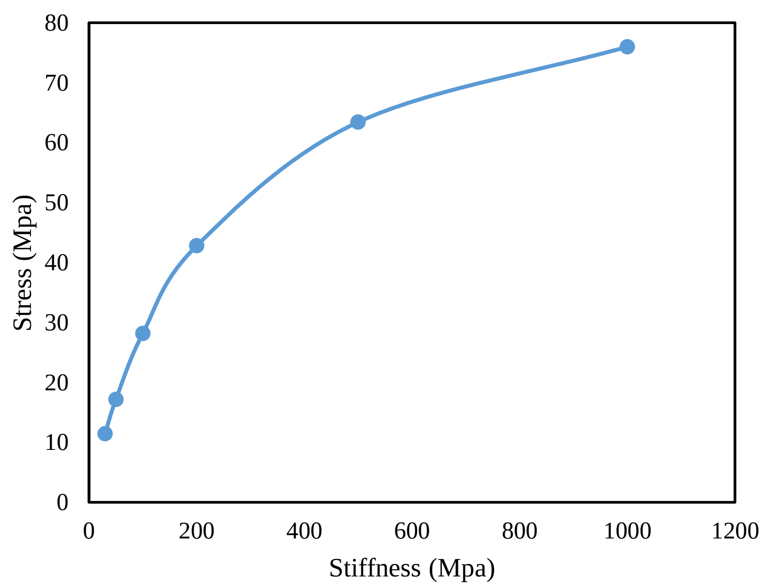

Figure 4- 18: Vertical stress development at the soil-pile interface with stiffness of soil

2. Stress Development with Increase in Temperature

For the analysis of stress development with the increase in temperature, an analysis was made with the increasing temperature from a very minimum of 3°C to an exceptionally maximum of 80°C and the relation was found to be directly proportional. From the graph of stress development vs change in temperature in the pile, it can be observed that the stress development is very rapid with the increment in temperature. The maximum developed stress was found to be 4.07 MPa while the temperature increment was 3^0C whereas within 80^0C in temperature increment, the developed stress was very large (93.504 MPa).

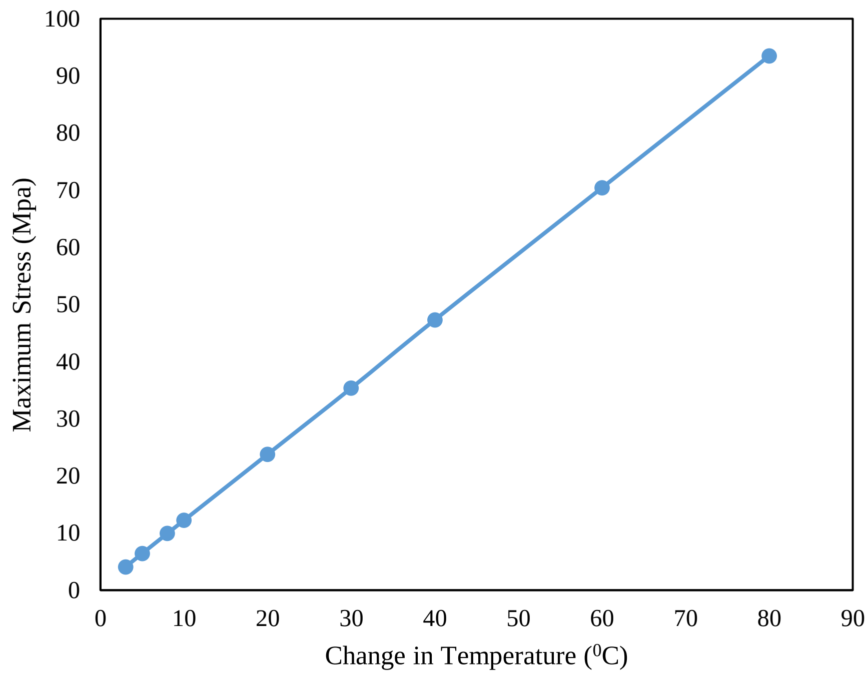

Figure 4- 19: Vertical stress development at the soil-pile interface with increase in temperature

3. Cooling Mode of Pile

Under the heating scenario of pile, a uniform temperature increment was applied in the pile foundation where the soil deposit and pile were set up at the constant temperature at the beginning of the simulation. Because of the heating effect on pile, soil surrounded by the pile faced compressive stress with a maximum value of the stress at about the mid-point of the pile because of the thermal friction produced during the application of heat on the pile from all the sides. On a different scenario when the pile was set to cool down from the initial temperature, a reverse scenario on the mechanical properties of the pile at the soil pile interface was observed as shown in figure 4-20. Moreover, due to the cooling of pile, the pile may experience shortening and may encounter a separation of the pile and soil from the bottom of the foundation, which is another part of the research and investigation in the future.

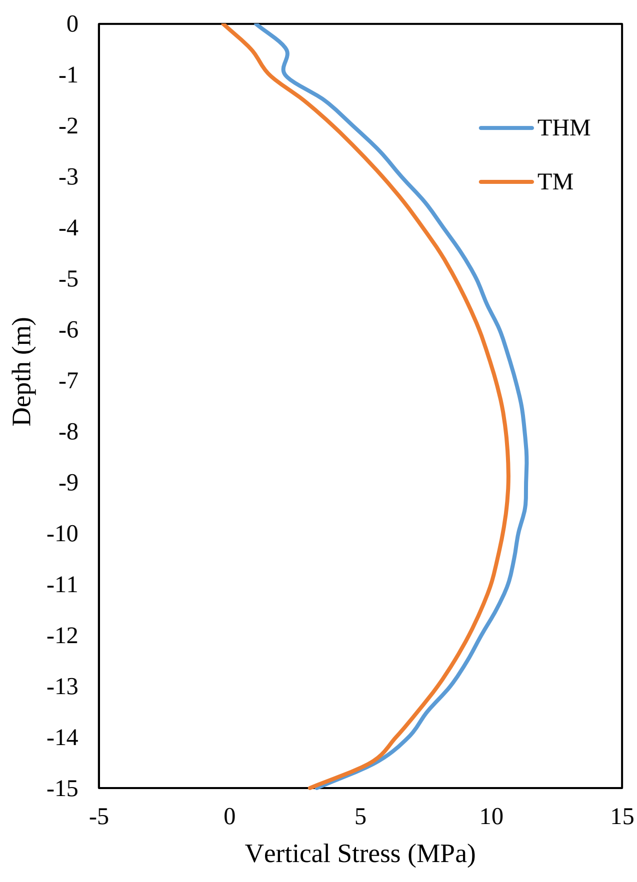

Figure 4- 20: Vertical stress variation at the soil pile interface during cooling mode of pile

4.7 Summary

The thermo-hydro-mechanical simulation of heat exchanger pile in three different conditions of loading was analyzed in this chapter and the results were analyzed accordingly. Two different scenarios of loading were applied during the saturated thermo-hydro-mechanical simulation which consists of either temperature constant with varying external mechanical load or temperature being changed with a constant value of mechanical load on the pile head and the third scenario was observed for the unsaturated condition of the soil in thermo-hydro-mechanical loading. There seems to be a larger change in the value of mechanical properties of pile i.e., stress, strain and displacement with the temperature increment as compared to load increment on the pile head. All the mechanical properties of the pile were found to be similar on both cases of loading except in the vertical displacement, which acts more as a mechanical loading scenario on the effect of temperature. Moreover, the stress development on the soil-pile interface was found to be increasing gradually with change in mechanical loading while keeping the temperature constant on the pile on each increased load. The vertical displacement, vertical stress and vertical strain were found to be increasing with the saturation on the soil. On the third approach of simulation in this chapter, unsaturated soil was considered and the analyzed results depict that the properties of the pile are affected by the unsaturation on the soil. On the other hand, the relation of stress development with the stiffness of soil is in gradual increment. There seemed to be larger stress development while the soil becomes stiffer from a loose soil but later on when the soil becomes stable the stress development was not varying as in the beginning stage. So what can be said is that, during the thermo-hydro-mechanical process, all the properties were found to be similar with the thermo-mechanical loading but with higher concentration on them i.e., vertical stress, vertical displacement and vertical strain all the parameters obtained were similar with thermo-mechanical loading but with higher value in case of thermo-hydro-mechanical loading. It can also be concluded that the thermal loading has more effects on the mechanical behavior of pile than the mechanical loading.

During the cooling mode of the pile, the stress, strain and displacement factors caused by coupled thermo-hydro-mechanical process were found to be in reverse nature than that of the heating mode of pile. Positive vertical stress in the soil pile interface was obtained during cooling mode of pile, whereas the vertical stress was found to be negative during the heating of the pile.

The shear stress around the soil pile interface occurs with maximum value at the ends of the pile, whereas it becomes minimum around the mid-section of the pile during TM and saturated THM condition and the shear stress variation becomes more abundant at the unsaturated region of soil during the simulation of unsaturated soil.

Chapter 5

Conclusion and Suggestions for Future work

5.1 Conclusion

Heat exchanger piles are “promising additions” to renewable energy which can be used to extract the ground source of heat energy to supply the heating or cooling of a building. This thesis presents some preliminary results on the behavior of a heat exchanger pile in finite element modeling.

A main part of the numerical investigation is devoted to the thermo-mechanical behavior of the heat exchanger pile. The expansion and contraction behavior during the heating and cooling cycles is studied. Scenarios such as free expansion in the absence of mechanical loads as well as combined thermal and mechanical loading are investigated. The vertical stress variation in the heat exchanger pile is symmetrical with the maximum stress value at nearly the mid depth of the pile in the free expansion case, for which the null point of the heat exchanger pile also lies at the mid-section of the pile if the pile is set to expand freely on both ends. When a mechanical load is applied to the top of pile while a temperature change is imposed, the shear stress was found to be maximum at the ends of the pile where the thermal expansion was maximum. The neutral point of a 15 m pile was found to be at 8.67 m from the top of the pile where the compressive vertical stress was maximum and the shear stress was changing from negative to positive. The influencing distance was determined by analyzing the effect of thermo-mechanical loading on the soil and found to be 3 m from the soil-pile interface of 1 m diameter pile.

The present study is also extended to address the behavior of the surrounding soil around the heat exchanger pile. The simulation of soil behavior is approached differently from the existing literature where the surrounding soil has been often treated as a dry material without consideration of the presence of water pressure or its evolution during the performance of the heat exchanger pile. Some preliminary simulations on the heat exchanger pile surrounded by either saturated or partially saturated soil are performed when coupled thermo-hydro-mechanical processes in the soil are considered. Overall, the behavior of the heat exchanger pile seems to remain similar to the earlier cases while the surrounding soil exhibits much more complicated characteristics, especially in the partially saturated zone which needs further investigation. The neutral point was found to be shifting by 0.04 m downwards in the simulation with thermos-hydro-mechanical loading as compared with the thermo-mechanical loading for a temperature difference of 10°C. From the analysis of vertical stress, horizontal stress, vertical displacement and vertical strains, the effect of loadings on the pile was found up to 4 m radially from the soil pile interface which was also considered as the influencing distance in the thermo-hydro-mechanical loading. The results found from the analysis of partially saturated soil were comparable with the results from the saturated condition in the fully saturated zone but in the region of partial saturation, the results were affected by the negative water pressure.

5.2 Suggestions for Future Work

The present study is primarily focused on the friction type of piles for which the load transfer is carried by the friction resistance of the soil. From a practice point of view, substantial research is still needed for the point bearing piles where the load is transferred to the underlying soils beneath the pile. In addition, the classical pile design models the friction resistance by the soil in a very different way than the elastic model explored in the presented numerical simulation. Incorporating the numerical results or findings of this research into the engineering practice demands significant further investigations.

The numerical modeling presented in this work encounters most of the challenges when dealing with partially saturated soils, whose behavior is very intricate and still a subject of intensive study. The present study utilizes a finite element program developed by a leading geotechnical group on the subject of partially saturated soils. However, continual refinement or improvement of the understanding and modeling of the constitutive behavior of partially saturated soils is still necessary for undertaking the modeling of complex multi-physics processes involved.

Many technical aspects of the presented numerical study can be also improved. More complicated hydraulic loading with water pressure or water flux changes on the surrounding soil needs to be studied. The effect of pile groups in different loading conditions can be studied. 2D analysis presented in this study can be extended to 3D modeling.

References

1. Code_Bright User's Guide, 2015
2. Ã, A.F.R.L. & Laloui, L.Ã., 2016. Thermally induced group effects among energy piles. , (2015).
3. Akrouch, G.A., Sánchez, M. & Briaud, J.-L., 2016. An experimental, analytical and numerical study on the thermal efficiency of energy piles in unsaturated soils. *Computers and Geotechnics*, 71, pp.207–220. Available at: http://www.sciencedirect.com/science/article/pii/S0266352X1500186X.
4. Amatya, B.L. et al., 2012. Thermo-mechanical behaviour of energy piles. *Géotechnique*, 62(6), pp.503–519.
5. Bourne-Webb, P.J. et al., 2009. Energy pile test at Lambeth College, London: geotechnical and thermodynamic aspects of pile response to heat cycles. *Géotechnique*, 59(3), pp.237–248.
6. Carotenuto, A., Massarotti, N. & Mauro, A., 2012. A new methodology for numerical simulation of geothermal down-hole heat exchangers. *Applied Thermal Engineering*, 48, pp.225–236. Available at: http://dx.doi.org/10.1016/j.applthermaleng.2012.04.021.
7. Gao, J. et al., 2008. Thermal performance and ground temperature of vertical pile-foundation heat exchangers: A case study. *Applied Thermal Engineering*, 28(17–18), pp.2295–2304.
8. Laloui, L., Nuth, M. & Vulliet, L., 2006. Experimental and numerical investigations of

the behaviour of a heat exchanger pile. *International Journal for Numerical and Analytical Methods in Geomechanics*, 30(8), pp.763–781.

9. Mimouni, T. & Laloui, L., 2015. Behaviour of a group of energy piles. *Canadian Geotechnical Journal*, 17(May), pp.1–17.
10. Ozudogru, T.Y., Olgun, C.G. & Arson, C.F., 2015. Analysis of Friction Induced Thermo-Mechanical Stresses on a Heat Exchanger Pile in Isothermal Soil. *Geotechnical and Geological Engineering*, 33(2), pp.357–371. Available at: http://dx.doi.org/10.1007/s10706-014-9821-0.
11. Rotta Loria, A.F. et al., 2015. Numerical modelling of energy piles in saturated sand subjected to thermo-mechanical loads. *Geomechanics for Energy and the Environment*, 1, pp.1–15. Available at: http://dx.doi.org/10.1016/j.gete.2015.03.002.
12. Suryatriyastuti, M.E., Mroueh, H. & Burlon, S., 2012. Understanding the temperature-induced mechanical behaviour of energy pile foundations. *Renewable and Sustainable Energy Reviews*, 16(5), pp.3344–3354. Available at: http://dx.doi.org/10.1016/j.rser.2012.02.062.
13. You, S. et al., 2014. In-situ experimental study of heat exchange capacity of CFG pile geothermal exchangers. *Energy and Buildings*, 79, pp.23–31. Available at: http://dx.doi.org/10.1016/j.enbuild.2014.04.021.
14. Rawal, K., Wang, Z. M., & Hu, L. B., Numerical Investigation of the Geomechanics of Sinkhole Formation and Subsidence, *In Geotechnical Frontiers 2017*, 480-487.
15. Rawal, K., Wang, Z. M., & Hu, L. B., Exploring the Geomechanics of Sinkholes: A Numerical Simulation Approach, *Geo-Chicago 2016*, 372.

16. Rawal, K., Wang, Z. M., & Hu, L. B., Exploring the Geomechanics of Sinkholes: A Numerical Study of Sinkhole Subsidence and Collapse, *In Geo-China 2016*, 1-8
17. Wang, Z. M., Yang, G. L., Yang, R. D., Rawal, K., & Hu, L. B., Evaluating the Factors Influencing Limestone-Dissolution Characteristics in the Karst Regions of Guizhou, China, *Journal of Testing and Evaluation*, 2016, *45*(1).
18. Wang, Z. M., Rawal, K., Hu, L. B., Yang, R. D., & Yang, G. L., A study of dissolution and water-bearing characteristics of the restricted platform dolomite facies in the karst areas of Guizhou, China, *Environmental Earth Sciences*, 2017, *76*(3), 124.

Appendix A

A.1 Model Preparation

The finite element analysis of Heat exchanger pile in Code_Bright starts with the modelling of a pile in a soil deposit. Here a 15 m deep and 0.5 m wide pile was modelled in a soil deposit of dimension 20 m X 20 m. NURBS surface should be assigned after the model creation so that we can apply our condition on the model. Here in the figure, Blue lines refer to the model lines whereas the pink lines are for NURBS surface.

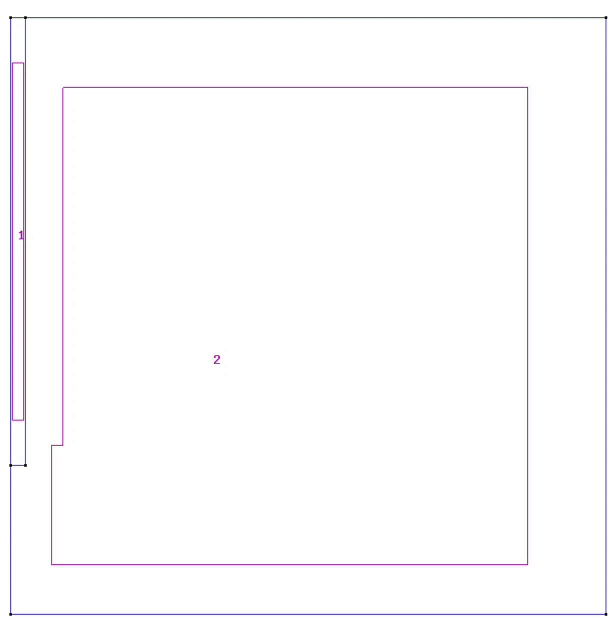

Figure A- 1: Heat Exchanger pile model

In the figure, Surface 1 represents the pile whereas surface 2 is for soil deposit around the pile.

On the second step of modelling a problem type should be defined to assign the required conditions and material properties. Here, Code_bright V_5.2 has been used.

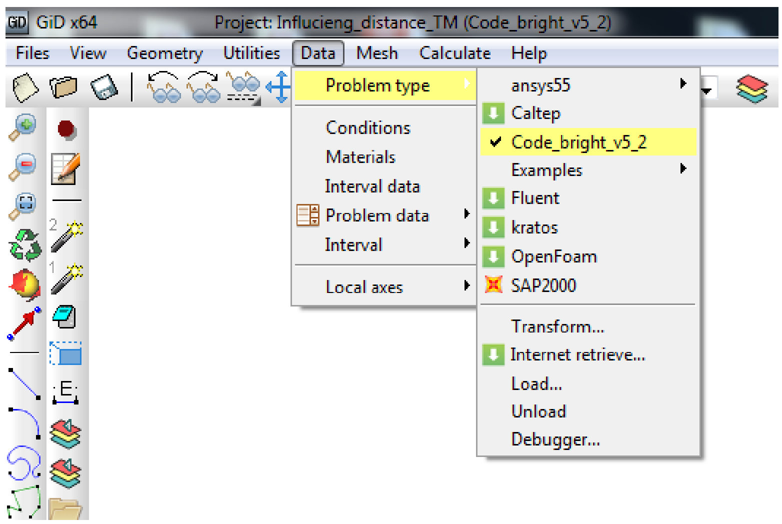

Figure A- 2: Defining Problem type

After the problem type, conditions, material properties, Interval Data and Problem data should be assigned per our requirement. As in Figure A-3, all the sides are constrained against expansion except on the top. Flux boundary condition is applied on surface 1 and Initial conditions are applied on surface 2 and initial porosity conditions are applied on both the surface 1 and 2 i.e., on concrete and soil.

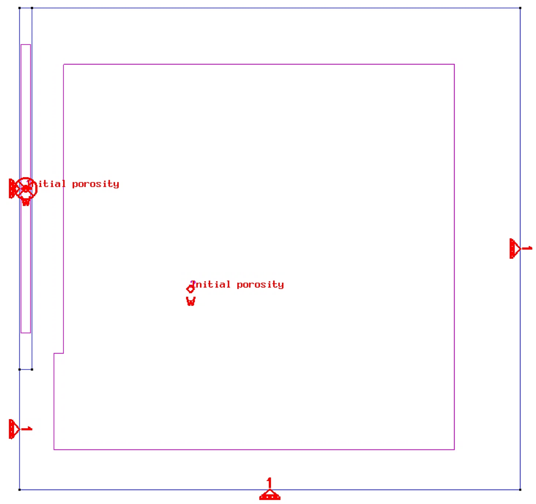

Figure A- 3: Applied Conditions

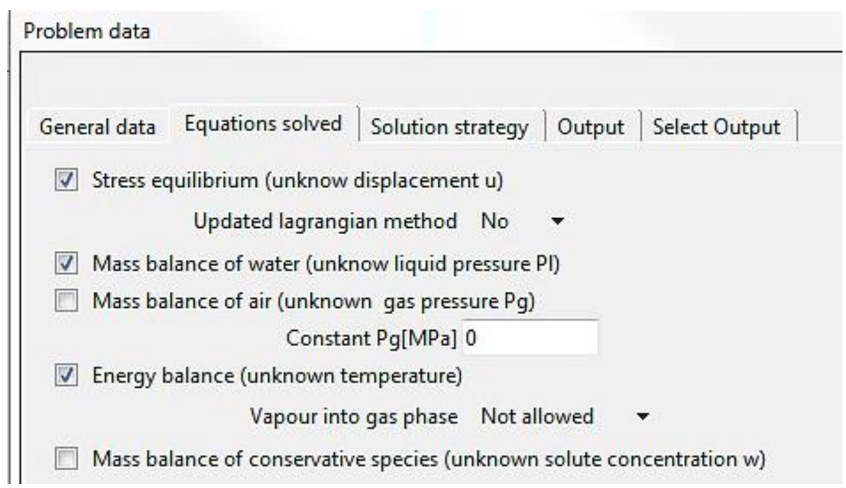

Figure A- 4: Defined Problem data

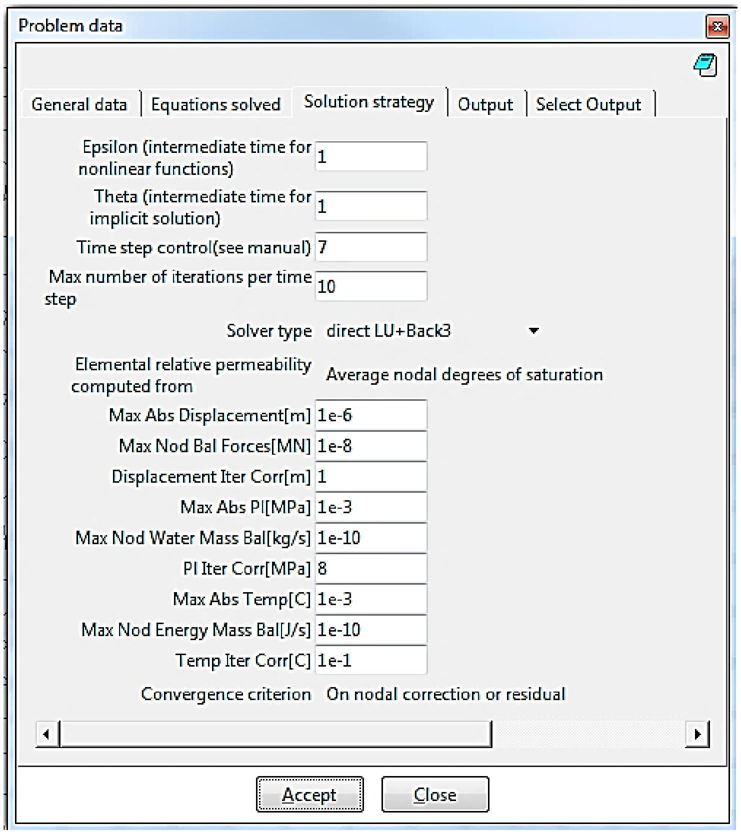

Figure A- 5: Defining Solver type and Correction values

Problem data are defined as per our requirements as in Figure A-4. Stress Equilibrium is for mechanical loadings; Mass balance of water is for hydraulic problems whereas the energy balance equation is for the thermal loadings. Here stress equilibrium, mass balance of water and energy balance equations are checked so that a coupled thermo-hydro-mechanical problem can be executed. Solution strategies, as in Figure A-5, are defined once the problem type are set up.

A.2 Define Material and Material Properties

The materials used in the modeling are defined so that their respective values are used as our requirement. Figure A-6 shows an example of defining material properties where the soil linear elastic properties are defined. Figure A-7 can shows all the materials in the model. Since soil and concrete are being used as the materials for this simulation, which are shown in Figure A-7.

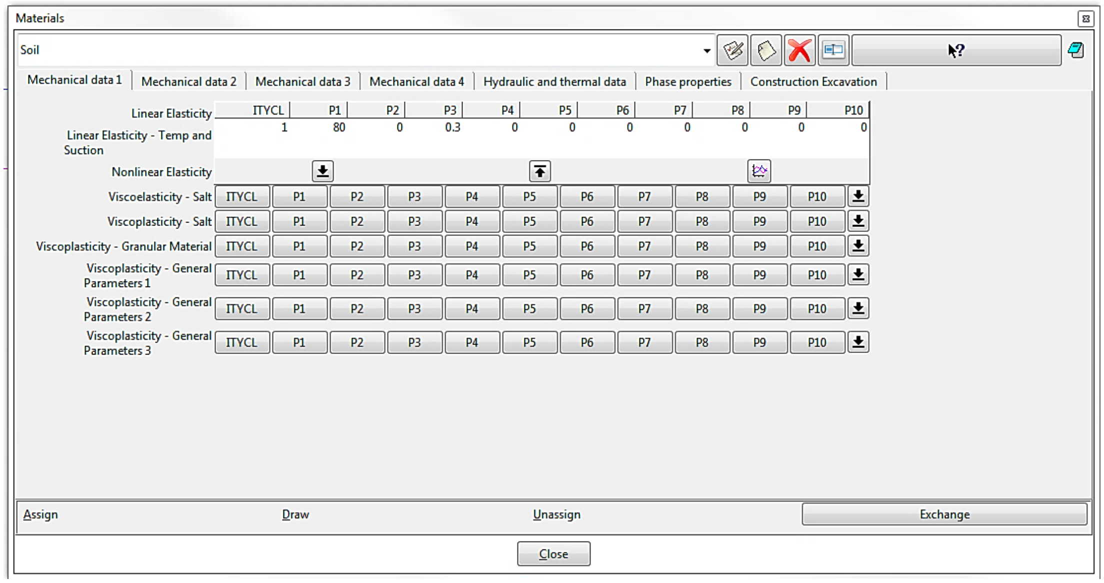

Figure A- 6: Defining soil properties

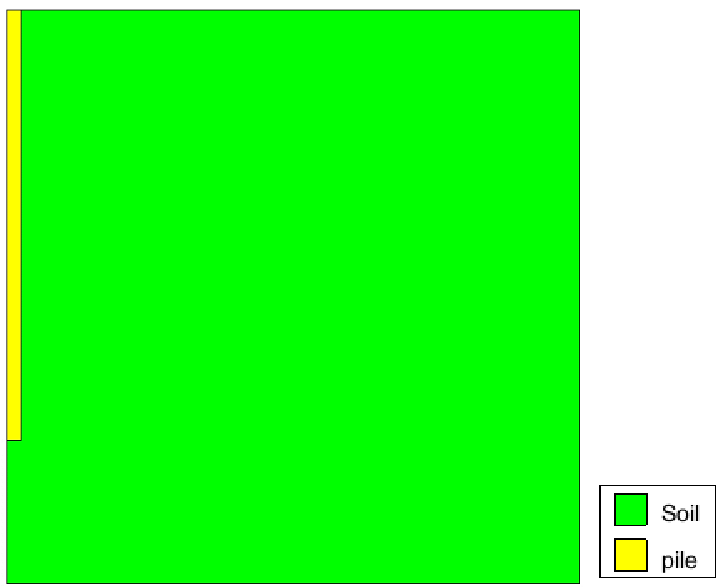

Figure A- 7: Material: soil and pile

A-3: Meshing

Both the structured and unstructured mesh can be generated in GID. In this thesis, unstructured meshing is used with quadratic elements. Here in the Figure A-8, it can be observed that the total number of elements and total number of nodes. Figure A-9 shows the model after meshing. The soil pile interface is more finely meshed whereas the soil deposit is coarse. Figs A-10, A-11 and A-12 are the output windows which are obtained after the calculation procedure. Figure A-10 shown the color map for the vertical stress variation along the model whereas in Figure A-12, a vertical stress distribution curve is plotted.

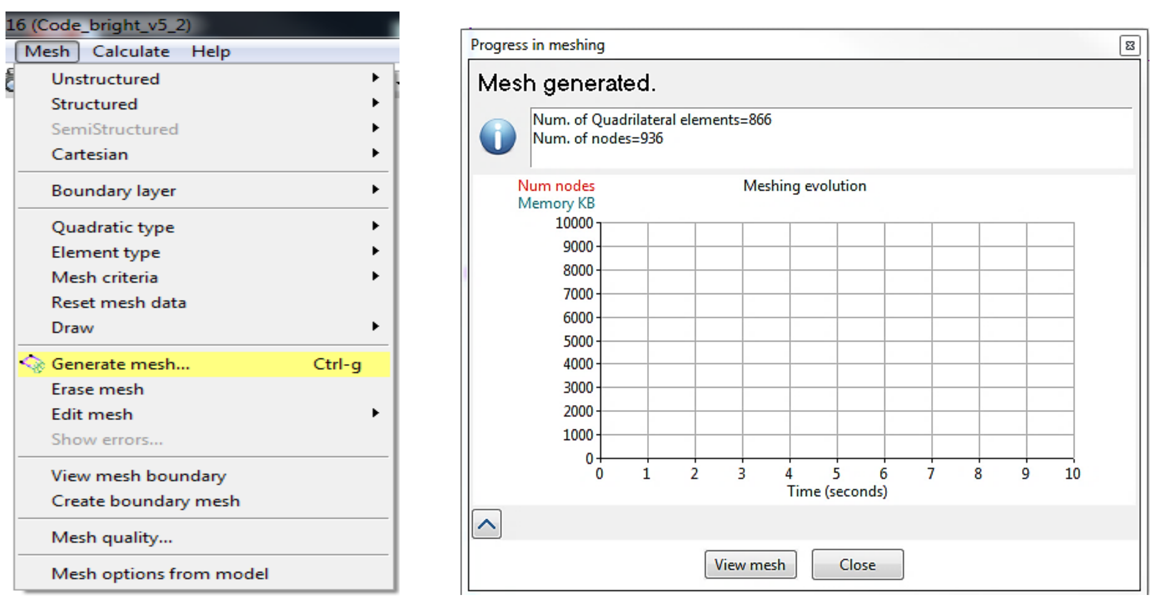

Figure A- 8: Mesh generation, Number of Nodes and Elements

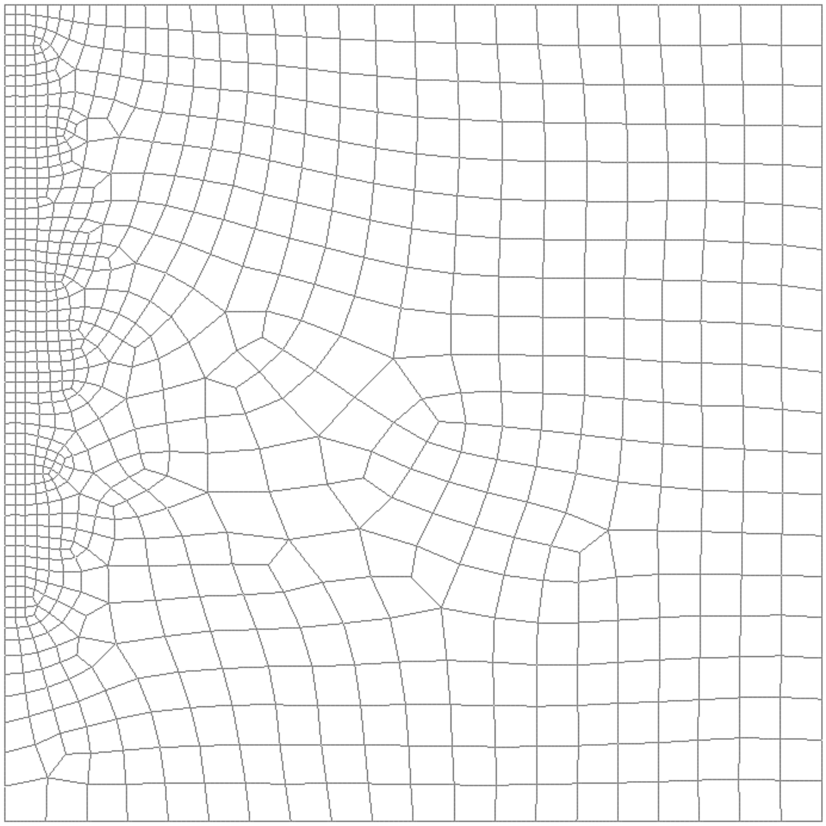

Figure A- 9: Generated Mesh

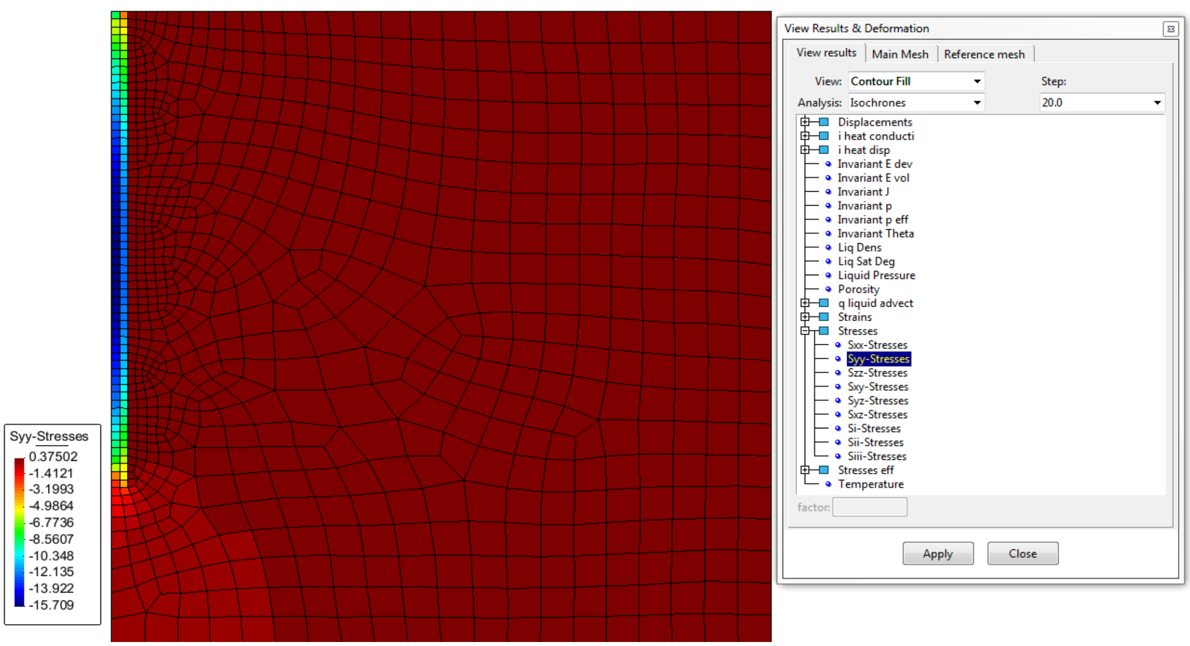

Figure A- 10: Vertical Stress Variation

A-4: Result Analysis

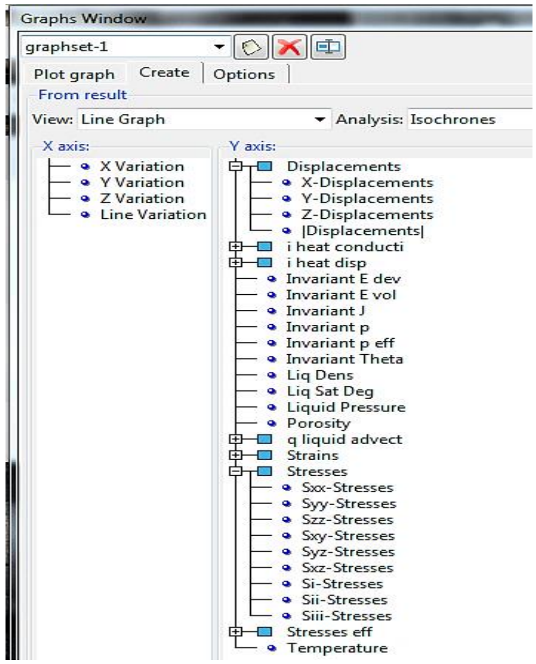

Figure A- 11: Results

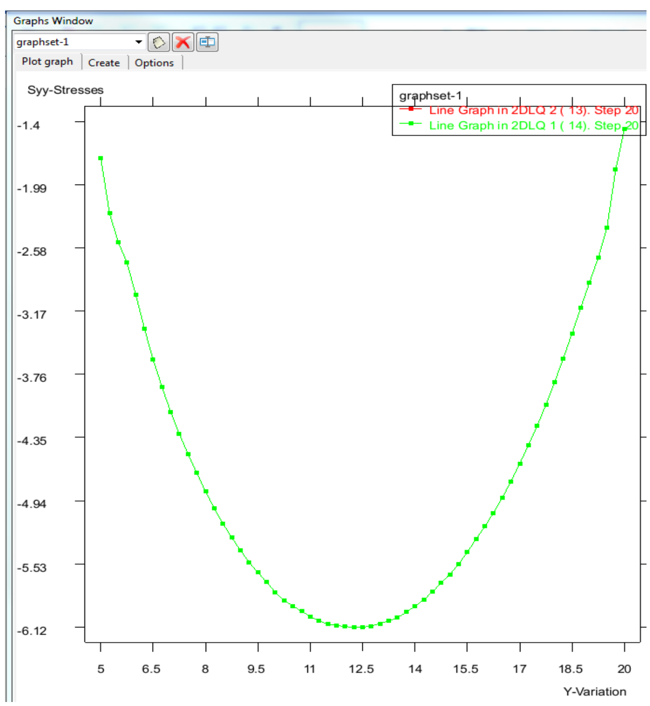

Figure A- 12: Vertical Stress Distribution